IEEE Access
Multidisciplinary | Rapid Review | Open Access Journal

Received June 9, 2018, accepted July 8, 2018, date of publication July 19, 2018, date of current version August 15, 2018.

Digital Object Identifier 10.1109/ACCESS.2018.2857496

Power Scaling Laws of Massive MIMO Full-Duplex Relaying With Hardware Impairments

SI-NIAN JIN[1], DIAN-WU YUE[1], (Senior Member, IEEE), AND HA H. NGUYEN[2], (Senior Member, IEEE)

[1]College of Information Science and Technology, Dalian Maritime University, Dalian 116026, China
[2]Department of Electrical and Computer Engineering, University of Saskatchewan, Saskatoon, SK S7N 5A9, Canada

Corresponding author: Dian-Wu Yue (dwyue@dlmu.edu.cn)

This work was supported in part by the Fundamental Research Funds for the Central Universities under Grant 3132016347 and in part by the Natural Science Foundation of Liaoning Province under Grant 201602086.

ABSTRACT This paper considers a massive MIMO full-duplex relaying (FDR) system, in which multiple single-antenna sources simultaneously communicate with multiple single-antenna destinations using a single relay that is equipped with $N_{\rm tx}$ transmit antennas and $N_{\rm rx}$ receive antennas. Under the practical scenario of imperfect channel-state information, the relay processes the received signals by means of maximum-ratio combining/maximum-ratio transmission (MRC/MRT) or zero-forcing (ZF) processing, and employs either the decode-and-forward (DF) or amplify-and-forward (AF) scheme. Considering hardware impairments, closed-form expressions of the lower bounds on the sum spectral efficiencies for DF and AF schemes are derived for both the MRC/MRT and ZF processing methods. Based on the obtained expressions, various power scaling laws are established to show the relationships among the transmit powers of the sources, relay, and pilots in order to maintain a desirable quality of service when $N_{\rm tx}$ and $N_{\rm rx}$ go to infinity but with a fixed ratio. In particular, it is found that the massive MIMO FDR systems under consideration are not affected by the loop interference, can save power, and improve the rate performance when the three transmit powers are scaled down to $1/N_{\rm rx}^a$, $1/N_{\rm tx}^b$, and $1/N_{\rm rx}^c$, respectively, where $a + c = 1$, $b + c < 1$, and $b > 0$. Numerical results corroborate the accuracy of the closed-form expressions and show that, when the loop interference level is small, using low-quality hardware at the relay and high-quality hardware at the sources and the destinations is a good design choice in the practical design of low-cost massive MIMO FDR systems.

INDEX TERMS Massive MIMO, full-duplex relaying, hardware impairments, decode-and-forward, amplify-and-forward, maximum-ratio combining, maximum-ratio transmission, zero-forcing, power scaling law.

I. INTRODUCTION

Considered as one of the most promising technologies for the next and future generations of cellular networks [1]–[5], massive MIMO is gaining a phenomenal attention from both industry and academia. Featuring up to hundreds of transmit/receive antennas, a massive MIMO system can provide a drastic increase in spectral and energy efficiencies [6]–[10]. With massive MIMO, each base station (BS) in a cellular network uses a very large antenna array to serve users with simple linear processing [3]. According to the law of large numbers, as the number of antennas tends to infinity, the fast fading effect, the intra-cell interference, and additive Gaussian noise can all be averaged out. On a parallel avenue, by conducting both transmission and reception at the same time and over the same frequency band, full-duplex relaying (FDR) is a powerful technique to reduce transmit power and substantially increase the spectral efficiency when compared to the conventional half-duplex relaying [11]–[14]. To take advantages of both these two key technologies, researchers have considered incorporating massive MIMO into FDR systems.

Performance analysis of various massive MIMO relaying systems has been carried out in [15]–[25]. In the context of massive MIMO relaying, the work presented in [15] gives a thorough secrecy performance analysis and makes a comparison between two classical relaying schemes, namely decode-and-forward (DF) and amplify-and-forward (AF). In [16] and [17], an achievable rate expression of the DF

scheme of a multipair massive MIMO FDR system is obtained analytically by using maximum-ratio combining/maximum-ratio transmission (MRC/MRT) or zero-forcing (ZF) processing. Furthermore, an interesting power scaling law is also presented. The performance analysis of one-way and two-way multipair AF FDR systems is studied in [18]–[20], which reveals that deploying a very large antenna array at the relay can eliminate the effect of loop interference if the transmit power of the relay is scaled down properly. Subsequently, Kong *et al.* [21], [22] demonstrate the impact of low-resolution analog-to-digital converters (ADCs) on a multipair AF massive MIMO system. The effect of spatial correlation on two-way FDR systems is considered in [23] and several power scaling laws under different scenarios are obtained. While most previous studies on massive MIMO relaying systems implicitly assume Rayleigh fading, the study in [24] and [25] investigates Rician fading. Furthermore, a low complexity power control scheme is proposed to optimize the spectral efficiencies in [25]. It should be pointed out, however, that all of studies discussed above consider massive MIMO relaying systems with ideal hardware. In contrast, the system of interest in this paper is a massive MIMO one-way relaying system operating in the more practical scenario of having transceiver hardware impairments.

Given that very large antenna arrays are employed in massive MIMO FDR systems, it is very desirable to be able to deploy inexpensive transceiver components in these systems. However, the inexpensive transceiver components usually cause serious hardware impairments (e.g., phase noise, power amplifier nonlinearity, low-noise amplifier nonlinearity, I/Q imbalance and ADC quantization noise), which must be considered in the practical design of massive MIMO FDR systems. Although the effects caused by hardware impairments can be mitigated by calibration and compensation to some extent, there always remain residual hardware impairments. A study on the impact of hardware impairments has been carried out for 5G networks incorporating the massive MIMO technique [26], [27]. It is shown that the residual hardware impairments can be modeled as an additive Gaussian impairment, whose variance depends on the power of the useful signal [26]–[33]. In particular, the aggregate effect of several hardware impairments originating from different sources in a massive MIMO system is studied in [26] by modelling the residual hardware impairments as additive distortion noises. Subsequently, Björnson *et al.* [27] present closed-form expressions of the achievable rate for the uplink of a massive MIMO system in which the hardware impairments are modelled as multiplicative phase noise and additive distortion noise.

Due to the practical relevance of massive MIMO FDR systems built with low-cost components, there has been growing interest in the study of massive MIMO FDR systems with hardware impairments [29]–[33]. Specifically, the FDR systems with hardware impairments can be used to help the users within the service range of the access points to improve their service quality and link capacity. In addition, they can also be used to extend the coverage to remote users beyond the service range of the access points. Thus they have been applied in several wireless network standards, e.g., LTE-A and IEEE 802.16j. In [29] and [30], approximate expressions of spectral efficiency of a multipair massive MIMO two-way relaying system with hardware impairments are obtained under perfect channel state information (CSI). Taking into account hardware impairments and with simple linear beamforming (BF) processing, Xia *et al.* [31] study a massive MIMO DF FDR system where sources/destinations are equipped with multiple antennas and propose a hardware-impairment-aware transceiver scheme (HIA scheme) to mitigate the distortion noises by exploiting the statistical channel knowledge and antenna arrays of sources/destinations. With MRC/MRT processing and considering hardware impairments, Xu *et al.* [32] and Xie *et al.* [33] investigate a massive MIMO DF FDR system and derive expressions of the achievable rate in the cases of perfect and imperfect CSI, respectively. They show that, as the number of antennas at the relay grows very large, the achievable rate is limited by hardware impairments at the sources and destinations rather than by hardware impairments at the relay or by other interference. Furthermore, a low complexity power control scheme is proposed to further improve the energy efficiency of MIMO DF FDR systems with hardware impairments in [33]. In general, power scaling is an important characteristic of any massive MIMO system since it indicates how the deployment of large-scale (massive) antenna arrays helps to scale down transmit power while maintaining system's target rate. The effect of power scaling on the massive MIMO FDR systems with hardware impairments has only been studied in [29], [30], [32], and [33], which focus on several specific situations. Specifically, Xie *et al.* [33] give performance analysis for a massive MIMO DF FDR system with MRC/MRT processing and hardware impairments under the practical scenario of imperfect CSI.

To the authors of best knowledge, with the exception of [33], there are no other studies on massive MIMO FDR systems with hardware impairments and under the realistic assumption of imperfect CSI. In particular, power scaling behaviors for massive MIMO FDR systems with hardware impairments and under imperfect CSI is little understood. Against this background and motivated by the facts that (i) ZF processing is another important and attractive linear processing in addition to MRC/MRT, and (ii) the signal processing complexity of AF is much lower than that of DF when implemented in a massive MIMO relay system [15], this paper investigates power scaling laws for massive MIMO FDR systems with MRC/MRT or ZF processing in DF and AF schemes under the scenario of imperfect CSI and hardware impairments. The main contributions of the paper are summarized as follows:

- With MRC/MRT or ZF processing, closed-form expressions for the lower bounds of the end-to-end achievable rates are derived for both DF and AF schemes in full-duplex mode. Since the lower bounds give very good

approximations of the achievable rates, these closed-form expressions are handy for system performance analysis and also help to establish various power scaling properties. Furthermore, these closed-form expressions obtained in the full-duplex mode can be readily modified to yield the achievable rates of massive MIMO DF or AF systems operating in the half-duplex mode with both MRC/MRT and ZF processing.

- It is shown that, when $N_{\rm tx}$ and $N_{\rm rx}$ grow unlimited, but with a fixed ratio, to maintain a desirable rate for DF and AF schemes with MRC/MRT or ZF processing, the transmit powers of the sources, relay and pilots can be scaled down to $1/N_{\rm rx}^a$, $1/N_{\rm tx}^b$ and $1/N_{\rm rx}^c$, respectively, where $a, b, c \geq 0, a+c \leq 1$ and $b+c \leq 1$. Furthermore, if $a+c=1$, $b+c<1$ and $b>0$, the effect of loop interference can be eliminated asymptotically, leading to better rate performance and higher energy saving. In addition, if $a+c<1$, $b+c<1$, $0 \leq a, b<1$ and $0<c<1$, the effect of hardware impairments of the relay can be eliminated, and the effect of hardware impairments of sources and destinations are the only factors that limit the system performance in both DF and AF strategies, while using the high-quality hardware at the sources and destinations helps to realize the great performance advantage of a massive MIMO FDR system.
- Numerical results indicate that, with a small loop interference level, using the high-quality hardware at the sources and destinations helps to improve the system performance much better than using the high-quality hardware at the relay. Compared to MRC/MRT processing, ZF processing obtains a greater performance improvement when high-quality hardware is used at the sources and destinations. On the other hand, with a high loop interference level, the hardware qualities at the sources and destinations have basically the same impact on the system performance as that of the hardware quality at the relay. In addition, numerical results show that power scaling in the relay's transmitter can suppress the impact of loop interference, hence not only can it save energy but also improve the system's rate performance. Finally, numerical results also show that the DF scheme can provide better rate performance than the AF scheme, and that MRC/MRT processing is able to suppress the loop interference better than ZF processing.

The remainder of this paper is organized as follows. Section II describes the massive MIMO FDR system model, channel estimation and transmission for both DF and AF schemes. Section III and Section IV derive the lower bounds on the achievable rate and give various power scaling laws with MRC/MRT or ZF processing for DF and AF schemes, respectively. Numerical results are presented in Section V. Section VI concludes the paper. Appendices provide derivations and proofs relevant to the analysis presented in the paper.

Notation: Boldface upper and lower case letters denote matrices and column vectors, respectively. The superscripts $(\cdot)^T$, $(\cdot)^*$ and $(\cdot)^H$ stand for transpose, conjugate and conjugate-transpose, respectively. $\mathbf{I}_N$ stands for $N \times N$ identity matrix. The expectation and the variance operators are denoted by $\mathbb{E}\{\cdot\}$ and $\mathbb{V}\text{ar}(\cdot)$, respectively. Finally, $\mathbf{Z} \sim \mathcal{CN}(\mathbf{0}, \mathbf{A})$ denotes a circularly-symmetric complex Gaussian vector $\mathbf{Z}$ with zero mean and covariance matrix $\mathbf{A}$.

II. SYSTEM MODEL

A. CHANNEL MODEL

The system under consideration is illustrated in Fig. 1, in which N source-destination pairs communicate with each other with the help of a full-duplex relay. Similar to [17], the application scenario of interest in this paper is such that the direct links among S_n and D_n do not exist due to large path loss and/or heavy shadowing. Specifically, source S_n wishes to communicate with destination D_n with the help of relay R, where $n \in \{1, \cdots, N\}$. It is assumed that each of the sources and destinations is equipped with a single antenna, while the receiving terminal and the transmitting terminal of the relay are equipped with $N_{\rm rx}$ and $N_{\rm tx}$ antennas, respectively.

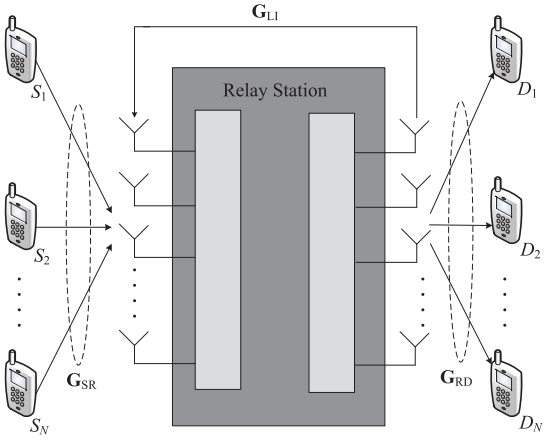

FIGURE 1. Full-duplex relaying with N source-destination pairs.

Let $\mathbf{G}_{\rm SR} \in \mathbb{C}^{N_{\rm rx} \times N}$ and $\mathbf{G}_{\rm RD} \in \mathbb{C}^{N_{\rm tx} \times N}$ represent the channel matrices from the sources to the receive antenna array of the relay station and from the destinations to the transmit antenna array of relay station, respectively. More specifically, $\mathbf{G}_\diamond, \diamond \in \{\text{SR, RD}\}$ is modelled as $\mathbf{G}_\diamond = \mathbf{H}_\diamond \mathbf{D}_\diamond^{1/2}$, where $\mathbf{H}_\diamond$ characterizes the small-scale fading whose entries are independent and identically distributed (i.i.d) $\mathcal{CN}(0, 1)$ random variables, and the diagonal matrix $\mathbf{D}_\diamond$ captures the large-scale fading whose nth diagonal element is denoted by $\beta_{\diamond,n}$ [6]. Moreover, the matrix $\mathbf{G}_{\rm LI} \in \mathbb{C}^{N_{\rm rx} \times N_{\rm tx}}$ represents the loop interference channel between the relay's transmit and receive arrays, whose entries are i.i.d. $\mathcal{CN}\left(0, \sigma_{\rm LI}^2\right)$ random variables.

B. CHANNEL ESTIMATION

In practice, the channels $\mathbf{G}_{\rm SR}$ and $\mathbf{G}_{\rm RD}$ need to be estimated at the relay station. To this end, all sources and destinations transmit their pilot sequences of length τ ($\tau \geq N$) symbols

to the relay station. The received matrices at the receive and transmit antenna arrays of the relay can be written as [17]

$$\mathbf{Y}_{\mathrm{r,P}} = \sqrt{P_{\mathrm{P}}}\mathbf{G}_{\mathrm{SR}}\Phi_{\mathrm{SR}} + \mathbf{G}_{\mathrm{SR}}\mathbf{N}_{\lambda,\mathrm{SR}} + \mathbf{N}_{\mu,\mathrm{SR}} + \mathbf{N}_{\mathrm{r,P}} \quad (1)$$

$$\mathbf{Y}_{\mathrm{t,P}} = \sqrt{P_{\mathrm{P}}}\mathbf{G}_{\mathrm{RD}}\Phi_{\mathrm{RD}} + \mathbf{G}_{\mathrm{RD}}\mathbf{N}_{\lambda,\mathrm{RD}} + \mathbf{N}_{\mu,\mathrm{RD}} + \mathbf{N}_{\mathrm{t,P}} \quad (2)$$

where P_{P} is the transmit power of uplink pilot symbols, $\mathbf{N}_{\mathrm{r,P}} \in \mathbb{C}^{N_{\mathrm{rx}}\times\tau}$ and $\mathbf{N}_{\mathrm{t,P}} \in \mathbb{C}^{N_{\mathrm{tx}}\times\tau}$ are additive white Gaussian noise (AWGN) matrices at the receive and transmit ends of the relay, respectively, and their entries are i.i.d. $\mathcal{CN}(0,1)$ random variables. Matrices $\Phi_{\mathrm{SR}} \in \mathbb{C}^{N\times\tau}$ and $\Phi_{\mathrm{RD}} \in \mathbb{C}^{N\times\tau}$ are uplink pilot matrices, which are built from the corresponding pilot sequences and can be chosen as discrete Fourier transform (DFT) matrices. The pairwise orthogonality of all pilot sequences means that $\Phi_{\mathrm{SR}}\Phi_{\mathrm{SR}}^H = \tau\mathbf{I}_N$ and $\Phi_{\mathrm{RD}}\Phi_{\mathrm{RD}}^H = \tau\mathbf{I}_N$ [34]. The matrices $\mathbf{N}_{\lambda,\mathrm{SR}} \in \mathbb{C}^{N\times\tau}$ and $\mathbf{N}_{\lambda,\mathrm{RD}} \in \mathbb{C}^{N\times\tau}$ represent the effects of imperfect transmit radio frequency (RF) chains [35], [36]. An important property is that the power of distortion noise at a given antenna is proportional to the signal power transmitted at this antenna. Therefore, the entries of $\mathbf{N}_{\lambda,\mathrm{SR}}$ and $\mathbf{N}_{\lambda,\mathrm{RD}}$ are i.i.d. $\mathcal{CN}(0,\lambda_{\mathrm{P}}P_{\mathrm{P}})$ random variables, where λ_{P} characterizes the level of transmit imperfection, which is assumed to be the same at sources and destinations. Similarly, $\mathbf{N}_{\mu,\mathrm{SR}} \in \mathbb{C}^{N_{\mathrm{rx}}\times\tau}$ and $\mathbf{N}_{\mu,\mathrm{RD}} \in \mathbb{C}^{N_{\mathrm{tx}}\times\tau}$ represent the effects of imperfect receive RF chains, whose entries are i.i.d. imperfect receive RF chains, whose entries are i.i.d. $\mathcal{CN}\left(0, \mu_{\mathrm{P}}\left(P_{\mathrm{P}}\left(1+\lambda_{\mathrm{P}}\right)\sum_{j=1}^{N}\beta_{\mathrm{SR},j}+1\right)\right)$ and $\mathcal{CN}\left(0, \mu_{\mathrm{P}}\left(P_{\mathrm{P}}\left(1+\lambda_{\mathrm{P}}\right)\sum_{j=1}^{N}\beta_{\mathrm{RD},j}+1\right)\right)$ random variables, respectively, where μ_{P} characterizes the level of receive imperfection [32], [33].

It is pointed out that existing results on pilot-based channel estimation [1], [17] apply for estimation of unknown channel corrupted by independent additive Gaussian noise with known statistics. However, such results do not apply to the considered model since the received pilot signals involve terms related to distortion noises, which are neither independent nor Gaussian distributed. More specifically, due to the presence of transmit distortion noises, the received pilot signals are degraded by the terms $\mathbf{G}_{\mathrm{SR}}\mathbf{N}_{\lambda,\mathrm{SR}}$ and $\mathbf{G}_{\mathrm{RD}}\mathbf{N}_{\lambda,\mathrm{RD}}$, which are not independent with the channel to be estimated. Moreover, $\mathbf{G}_{\mathrm{SR}}\mathbf{N}_{\lambda,\mathrm{SR}}$ and $\mathbf{G}_{\mathrm{RD}}\mathbf{N}_{\lambda,\mathrm{RD}}$ are products of Gaussian random variables, thus they are actually non-Gaussian.

Because the linear minimum mean square-error (LMMSE) estimation (see [26], [27]) is relatively complicated, and is not conducive to the system analysis, this paper adopts the linear least-square (LS) estimation for convenience. The LS estimation of $\mathbf{G}_{\mathrm{SR}}$ and $\mathbf{G}_{\mathrm{RD}}$ can be written as [34]

$$\hat{\mathbf{G}}_{\mathrm{SR}} = \frac{\mathbf{Y}_{\mathrm{r,P}}\Phi_{\mathrm{SR}}^H}{\tau\sqrt{P_{\mathrm{P}}}} \quad (3)$$

$$\hat{\mathbf{G}}_{\mathrm{RD}} = \frac{\mathbf{Y}_{\mathrm{t,P}}\Phi_{\mathrm{RD}}^H}{\tau\sqrt{P_{\mathrm{P}}}}. \quad (4)$$

For the nth column vectors of $\hat{\mathbf{G}}_{\mathrm{SR}}$ and $\hat{\mathbf{G}}_{\mathrm{RD}}$, they are distributed as $\hat{\mathbf{g}}_{\mathrm{SR},n} \sim \mathcal{CN}\left(\mathbf{0}, \sigma_{\mathrm{SR},n}^2\mathbf{I}_{N_{\mathrm{rx}}}\right)$ and $\hat{\mathbf{g}}_{\mathrm{RD},n} \sim \mathcal{CN}\left(\mathbf{0}, \sigma_{\mathrm{RD},n}^2\mathbf{I}_{N_{\mathrm{tx}}}\right)$, where

$$\sigma_{\mathrm{SR},n}^2 = \beta_{\mathrm{SR},n} + \frac{\lambda_{\mathrm{P}}+\mu_{\mathrm{P}}+\lambda_{\mathrm{P}}\mu_{\mathrm{P}}}{\tau}\sum_{j=1}^{N}\beta_{\mathrm{SR},j} + \frac{\mu_{\mathrm{P}}+1}{\tau P_{\mathrm{P}}} \quad (5)$$

$$\sigma_{\mathrm{RD},n}^2 = \beta_{\mathrm{RD},n} + \frac{\lambda_{\mathrm{P}}+\mu_{\mathrm{P}}+\lambda_{\mathrm{P}}\mu_{\mathrm{P}}}{\tau}\sum_{j=1}^{N}\beta_{\mathrm{RD},j} + \frac{\mu_{\mathrm{P}}+1}{\tau P_{\mathrm{P}}}. \quad (6)$$

Unlike the analysis under perfect CSI assumption, the non-Gaussian distortion noise caused by hardware impairments needs to be taken into account in the system performance analysis and this is done in Sections III and IV.

C. DF DATA TRANSMISSION

At time instant i, all sources transmit their signals $\mathbf{x}[i]$ to the relay station, while the relay broadcasts $\mathbf{s}[i]$ to destinations under the DF strategy. The received signals at the relay station and the N destinations are given by [32]

$$\begin{aligned}\mathbf{y}_{\mathrm{R}}[i] = {} & \sqrt{P_{\mathrm{S}}}\mathbf{G}_{\mathrm{SR}}\mathbf{x}[i] + \mathbf{G}_{\mathrm{SR}}\mathbf{n}_1[i] + \sqrt{P_{\mathrm{R}}}\mathbf{G}_{\mathrm{LI}}\mathbf{s}[i] \\ & + \mathbf{G}_{\mathrm{LI}}\mathbf{n}_3[i] + \mathbf{n}_2[i] + \mathbf{n}_{\mathrm{R}}[i] \quad (7)\end{aligned}$$

$$\mathbf{y}_{\mathrm{D}}[i] = \sqrt{P_{\mathrm{R}}}\mathbf{G}_{\mathrm{RD}}^T\mathbf{s}[i] + \mathbf{G}_{\mathrm{RD}}^T\mathbf{n}_3[i] + \mathbf{n}_4[i] + \mathbf{n}_{\mathrm{D}}[i] \quad (8)$$

where P_{S} and P_{R} are the transmit powers of each source and of the relay station, respectively. The signals are modelled as $\mathbf{x}[i] \sim \mathcal{CN}(\mathbf{0}, \mathbf{I}_N)$, whereas $\mathbf{n}_{\mathrm{R}}[i] \sim \mathcal{CN}\left(\mathbf{0}, \mathbf{I}_{N_{\mathrm{rx}}}\right)$ and $\mathbf{n}_{\mathrm{D}}[i] \sim \mathcal{CN}(\mathbf{0}, \mathbf{I}_N)$ denote AWGN vectors at the relay's receiver and destinations, respectively. The vectors $\mathbf{n}_1[i]$, $\mathbf{n}_2[i]$, $\mathbf{n}_3[i]$ and $\mathbf{n}_4[i]$ denote the distortion noises of sources, the relay's receiver, the relay's transmitter and destinations, respectively. The distortion noises caused by imperfect RF chains can be represented as

$$n_{1,n}[i] \sim \mathcal{CN}(0, \delta_{1,n}), \quad \delta_{1,n} = \lambda_1 P_{\mathrm{S}}\mathbb{E}\left\{|x_n[i]|^2\right\} \quad (9)$$

$$n_{2,m}[i] \sim \mathcal{CN}(0, \delta_{2,m}), \quad \delta_{2,m} = \mu_1\mathbb{E}\left\{\left|y_{\mathrm{R},m}[i]\right|^2\right\} \quad (10)$$

$$n_{3,m}[i] \sim \mathcal{CN}(0, \delta_{3,m}), \quad \delta_{3,m} = \lambda_2 P_{\mathrm{R}}\mathbb{E}\left\{|s_m[i]|^2\right\} \quad (11)$$

$$n_{4,n}[i] \sim \mathcal{CN}(0, \delta_{4,n}), \quad \delta_{4,n} = \mu_2\mathbb{E}\left\{\left|y_{\mathrm{D},n}[i]\right|^2\right\} \quad (12)$$

where λ_1 and λ_2 characterize the levels of transmit imperfection of sources and the relay's transmitter, respectively. Likewise, μ_1 and μ_2 characterize the levels of receive imperfection of the relay's receiver and destinations, respectively. The quantities $x_n[i]$, $y_{\mathrm{D},n}[i]$, $n_{1,n}[i]$ and $n_{4,n}[i]$ are the nth elements of $\mathbf{x}[i]$, $\mathbf{y}_{\mathrm{D}}[i]$, $\mathbf{n}_1[i]$ and $\mathbf{n}_4[i]$, respectively. Similarly, $y_{\mathrm{R},m}[i]$, $s_m[i]$, $n_{2,m}[i]$ and $n_{3,m}[i]$ are the mth elements of $\mathbf{y}_{\mathrm{R}}[i]$, $\mathbf{s}[i]$, $\mathbf{n}_2[i]$ and $\mathbf{n}_3[i]$, respectively. Lastly, $\mathbf{s}[i]$ represents the signals forwarded by the relay to destinations. The expression for $\mathbf{s}[i]$ depends on the linear processing adopted at the relay and are detailed next for the cases of MRC/MRT and ZF processing.

1) LINEAR RECEIVER

With a linear receiver, the received signal $\mathbf{y}_{\mathrm{R}}[i]$ is separated into N streams by multiplying with matrix $\mathbf{W}^H$ as follows [32]:

$$\mathbf{r}[i] = \mathbf{W}^H \mathbf{y}_{\mathrm{R}}[i]. \tag{13}$$

The relay then uses the nth stream (i.e., the nth element of $\mathbf{r}[i]$) to decode the signal transmitted from S_n. The nth element of $\mathbf{r}[i]$ can be expressed as

$$\begin{aligned} r_n[i] = {} & \sqrt{P_{\mathrm{S}}}\mathbf{w}_n^H \mathbf{g}_{\mathrm{SR},n} x_n[i] + \sqrt{P_{\mathrm{S}}} \sum_{j\neq n}^{N} \mathbf{w}_n^H \mathbf{g}_{\mathrm{SR},j} x_j[i] \\ & + \sum_{j=1}^{N} \mathbf{w}_n^H \mathbf{g}_{\mathrm{SR},j} n_{1,j}[i] + \sqrt{P_{\mathrm{R}}}\mathbf{w}_n^H \mathbf{G}_{\mathrm{LI}} \mathbf{s}[i] \\ & + \mathbf{w}_n^H \mathbf{G}_{\mathrm{LI}} \mathbf{n}_3[i] + \mathbf{w}_n^H \mathbf{n}_2[i] + \mathbf{w}_n^H \mathbf{n}_{\mathrm{R}}[i] \end{aligned} \tag{14}$$

where $\mathbf{g}_{\mathrm{SR},n}$ and $\mathbf{w}_n$ are the nth columns of $\mathbf{G}_{\mathrm{SR}}$ and $\mathbf{W}$, respectively. The MRC and ZF receivers that are of interest in this paper correspond to $\mathbf{W} = \hat{\mathbf{G}}_{\mathrm{SR}}$ and $\mathbf{W} = \hat{\mathbf{G}}_{\mathrm{SR}}\left(\hat{\mathbf{G}}_{\mathrm{SR}}^H \hat{\mathbf{G}}_{\mathrm{SR}}\right)^{-1}$, respectively.

2) LINEAR PRECODING

With the DF strategy, the relay first detects the transmitted signals from sources. It then performs linear precoding on these detected signals and forward the results to destinations. Assuming perfect detection at the relay and taking into account processing delay [17], the transmit signals at the relay are precoded versions of $\mathbf{x}[i-d]$, where d represents the processing delay. It is assumed that $d \geq 1$, which guarantees that, for a given time instant, the receive and transmit signals at the relay station are uncorrelated. Hence the forwarded signals at the relay are given as $\mathbf{s}[i] = \mathbf{A}\mathbf{x}[i-d]$, where $\mathbf{A}$ is the linear precoding matrix at the relay station. For MRT precoding, one has $\mathbf{A} = \alpha_{\mathrm{MRT}}\hat{\mathbf{G}}_{\mathrm{RD}}^*$, whereas $\mathbf{A} = \alpha_{\mathrm{ZF}}\hat{\mathbf{G}}_{\mathrm{RD}}^*\left(\hat{\mathbf{G}}_{\mathrm{RD}}^T\hat{\mathbf{G}}_{\mathrm{RD}}^*\right)^{-1}$ for ZF precoding. The value of α_{MRT} and α_{ZF} are chosen to satisfy a long-term total transmit power constraint at the relay, i.e., $\mathbb{E}\left\{\|\mathbf{s}[i]\|^2\right\} = 1$. For MRT precoding, one has [17] $\alpha_{\mathrm{MRT}} = 1/\sqrt{N_{\mathrm{tx}}\sum_{j=1}^{N}\sigma_{\mathrm{RD},j}^2}$. On the other hand, $\alpha_{\mathrm{ZF}} = 1/\sqrt{\sum_{j=1}^{N}\varphi_{\mathrm{RD},j}}$, where

$$\eta_{\diamond,i} = \beta_{\diamond,i} + \frac{\mu_{\mathrm{P}} + \lambda_{\mathrm{P}}\mu_{\mathrm{P}}}{\tau}\sum_{k=1}^{N}\beta_{\diamond,k} + \frac{\mu_{\mathrm{P}}+1}{\tau P_{\mathrm{P}}} \tag{15}$$

$$\theta_{\diamond,i} = \frac{\beta_{\diamond,i}}{\eta_{\diamond,i}} \tag{16}$$

$$\varepsilon_{\diamond,i} = \beta_{\diamond,i} - \frac{\beta_{\diamond,i}^2}{\eta_{\diamond,i}} \tag{17}$$

$$\varphi_{\diamond,i} = \frac{\tau + \lambda_{\mathrm{P}}\eta_{\diamond,i}\theta_{\diamond,i}^2\sum_{l=1}^{N}\eta_{\diamond,l}^{-1}}{(N_\diamond - N)\,\tau\eta_{\diamond,i}} + \frac{\lambda_{\mathrm{P}}\sum_{l=1}^{N}\eta_{\diamond,l}^{-1}\sum_{l=1}^{N}\varepsilon_{\diamond,l}}{(N_\diamond - N)^2\tau\eta_{\diamond,i}}. \tag{18}$$

In (15) to (18), we define $\diamond \in \{\mathrm{SR}, \mathrm{RD}\}$ and $i \in \{1, \cdots, N\}$. When $\diamond \equiv \mathrm{SR}$, $N_\diamond = N_{\mathrm{rx}}$, whereas $N_\diamond = N_{\mathrm{tx}}$ when $\diamond \equiv \mathrm{RD}$. The derivation of α_{ZF} is given in Appendix B.

From (8), the received signal at D_n can be expressed as [32]:

$$\begin{aligned} y_{\mathrm{D},n}[i] = {} & \sqrt{P_{\mathrm{R}}}\mathbf{g}_{\mathrm{RD},n}^T \mathbf{a}_n x_n[i-d] + \sqrt{P_{\mathrm{R}}}\sum_{j\neq n}^{N}\mathbf{g}_{\mathrm{RD},n}^T\mathbf{a}_j \\ & \times x_j[i-d] + \mathbf{g}_{\mathrm{RD},n}^T\mathbf{n}_3[i] + n_{4,n}[i] + n_{\mathrm{D},n}[i] \end{aligned} \tag{19}$$

where $\mathbf{g}_{\mathrm{RD},n}$ and $\mathbf{a}_n$ are the nth columns of $\mathbf{G}_{\mathrm{RD}}$ and $\mathbf{A}$, respectively, and $n_{\mathrm{D},n}[i]$ is the nth element of $\mathbf{n}_{\mathrm{D}}[i]$.

D. AF DATA TRANSMISSION

Similar to (7) in the case of DF strategy, the received signal vector at the relay under AF strategy is formulated as [18]

$$\begin{aligned} \mathbf{y}_{\mathrm{R}}[i] = {} & \sqrt{P_{\mathrm{S}}}\mathbf{G}_{\mathrm{SR}}\mathbf{x}[i] + \mathbf{G}_{\mathrm{SR}}\mathbf{n}_1[i] + \mathbf{G}_{\mathrm{LI}}\mathbf{y}_{\mathrm{RT}}[i] \\ & + \mathbf{G}_{\mathrm{LI}}\mathbf{n}_3[i] + \mathbf{n}_2[i] + \mathbf{n}_{\mathrm{R}}[i] \end{aligned} \tag{20}$$

where $\mathbf{y}_{\mathrm{RT}}[i] \in \mathbb{C}^{N_{\mathrm{tx}}\times 1}$ denotes the transmitted signal vector at the relay station. With AF strategy, this signal vector is

$$\mathbf{y}_{\mathrm{RT}}[i] = \sqrt{P_{\mathrm{R}}}\rho\mathbf{F}\mathbf{y}_{\mathrm{R}}[i-1] \tag{21}$$

where $\mathbf{y}_{\mathrm{R}}[i-1]$ is simply the signal vector received previously at the relay [18], $\mathbf{F} = \hat{\mathbf{G}}_{\mathrm{RD}}^*\hat{\mathbf{G}}_{\mathrm{SR}}^H$ and $\mathbf{F} = \hat{\mathbf{G}}_{\mathrm{RD}}^*\left(\hat{\mathbf{G}}_{\mathrm{RD}}^T\hat{\mathbf{G}}_{\mathrm{RD}}^*\right)^{-1}\left(\hat{\mathbf{G}}_{\mathrm{SR}}^H\hat{\mathbf{G}}_{\mathrm{SR}}\right)^{-1}\hat{\mathbf{G}}_{\mathrm{SR}}^H$ represent the MRC/MRT and ZF processing matrices at the relay, respectively, and ρ is the power amplification factor.

To reduce processing complexity, a fixed gain is employed [18]. Define $\mathbf{y}_{\mathrm{RT}}[i-1] = \sqrt{P_{\mathrm{R}}}\tilde{\mathbf{y}}_{\mathrm{RT}}[i-1]$. For convenience of analysis, assume that pre-suppression techniques are employed [37] to yield the approximation $\tilde{\mathbf{y}}_{\mathrm{RT}}[i-1] \sim \mathcal{CN}(0, \frac{1}{N_{\mathrm{tx}}}\mathbf{I}_{N_{\mathrm{tx}}})$. Thus the received signal vector at D_n is given in (22), as show at the bottom of this page.

$$\begin{aligned} y_{\mathrm{D},n}[i] = {} & \rho\sqrt{P_{\mathrm{S}}P_{\mathrm{R}}}\mathbf{g}_{\mathrm{RD},n}^T\mathbf{F}\mathbf{g}_{\mathrm{SR},n}x_n[i-1] + \rho\sqrt{P_{\mathrm{S}}P_{\mathrm{R}}}\sum_{j\neq n}^{N}\mathbf{g}_{\mathrm{RD},n}^T\mathbf{F}\mathbf{g}_{\mathrm{SR},j}x_j[i-1] \\ & + \rho\sqrt{P_{\mathrm{R}}}\mathbf{g}_{\mathrm{RD},n}^T\mathbf{F}\mathbf{G}_{\mathrm{SR}}\mathbf{n}_1[i-1] + \rho P_{\mathrm{R}}\mathbf{g}_{\mathrm{RD},n}^T\mathbf{F}\mathbf{G}_{\mathrm{LI}}\tilde{\mathbf{y}}_{\mathrm{RT}}[i-1] + \rho\sqrt{P_{\mathrm{R}}}\mathbf{g}_{\mathrm{RD},n}^T\mathbf{F}\mathbf{G}_{\mathrm{LI}}\mathbf{n}_3[i-1] \\ & + \rho\sqrt{P_{\mathrm{R}}}\mathbf{g}_{\mathrm{RD},n}^T\mathbf{F}\mathbf{n}_{\mathrm{R}}[i-1] + \rho\sqrt{P_{\mathrm{R}}}\mathbf{g}_{\mathrm{RD},n}^T\mathbf{F}\mathbf{n}_2[i-1] + \mathbf{g}_{\mathrm{RD},n}^T\mathbf{n}_3[i] + n_{\mathrm{D},n}[i] + n_{4,n}[i] \end{aligned} \tag{22}$$

It follows that the value of ρ that satisfies the power constraint $\mathbb{E}\left\{\|\mathbf{y}_{\mathrm{RT}}[i]\|^2\right\} = P_{\mathrm{R}}$ is given as

$$\rho = \sqrt{\frac{1}{\mathbb{E}\left\{\begin{array}{l} P_{\mathrm{S}}\|\mathbf{F}\mathbf{G}_{\mathrm{SR}}\|^2 + P_{\mathrm{R}}\left\|\mathbf{F}\mathbf{G}_{\mathrm{LI}}\tilde{\mathbf{y}}_{\mathrm{RT}}[i-1]\right\|^2 \\ +\|\mathbf{F}\mathbf{G}_{\mathrm{SR}}\mathbf{n}_1[i-1]\|^2 + \|\mathbf{F}\mathbf{n}_2[i-1]\|^2 \\ +\|\mathbf{F}\mathbf{G}_{\mathrm{LI}}\mathbf{n}_3[i-1]\|^2 + \|\mathbf{F}\mathbf{n}_{\mathrm{R}}[i-1]\|^2 \end{array}\right\}}}. \quad (23)$$

III. ACHIEVABLE RATE ANALYSIS AND POWER SCALING LAWS WITH THE DF Protocol

A. DF ACHIEVABLE RATE ANALYSIS

In this section, with MRC/MRT or ZF processing, we derive the sum spectral efficiency of DF strategy in the full-duplex mode. The achievable rate is limited by the weakest/bottleneck link, i.e., it is equal to the minimum of the achievable rates of the transmissions from S_n to R and from R to D_n. By using a technique from [17], the received signal at the relay's receiver or at destination is rewritten as a known mean gain times the desired symbol, plus the uncorrelated effective noise which can be equivalent to independent Gaussian noise of the same variance in the worst case. Furthermore, since the effective noise is a sum of many terms, according to the central limit theorem, the Gaussian noise approximation should be very accurate, especially for massive MIMO systems. This technique is very suitable for analyzing the massive MIMO systems since: (i) it yields a simplified insightful rate expression, which is basically a lower bound of what can be achieved in practice; and (ii) it only require statistical CSI at the terminal [17], [38], [39].

First, we analyze the link from S_n to R by this technique. From (14), the received signal used for detecting $x_n[i]$ at the relay station can be written as

$$r_n[i] = \underbrace{\sqrt{P_{\mathrm{S}}}\mathbb{E}\left\{\mathbf{w}_n^H\mathbf{g}_{\mathrm{SR},n}\right\}x_n[i]}_{\text{desired signal}} + \underbrace{\tilde{n}_{\mathrm{R},n}[i]}_{\text{effective noise}} \quad (24)$$

where the effective noise $\tilde{n}_{\mathrm{R},n}[i]$ is given by

$$\begin{aligned}\tilde{n}_{\mathrm{R},n}[i] &= \sqrt{P_{\mathrm{S}}}\left(\mathbf{w}_n^H\mathbf{g}_{\mathrm{SR},n} - \mathbb{E}\left\{\mathbf{w}_n^H\mathbf{g}_{\mathrm{SR},n}\right\}\right)x_n[i] \\ &+ \sqrt{P_{\mathrm{S}}}\sum_{j\neq n}^{N}\mathbf{w}_n^H\mathbf{g}_{\mathrm{SR},j}x_j[i] + \sum_{j=1}^{N}\mathbf{w}_n^H\mathbf{g}_{\mathrm{SR},j}n_{1,j}[i] + \sqrt{P_{\mathrm{R}}} \\ &\mathbf{w}_n^H\mathbf{G}_{\mathrm{LI}}\mathbf{s}[i] + \mathbf{w}_n^H\mathbf{G}_{\mathrm{LI}}\mathbf{n}_3[i] + \mathbf{w}_n^H\mathbf{n}_2[i] + \mathbf{w}_n^H\mathbf{n}_{\mathrm{R}}[i]. \quad (25)\end{aligned}$$

Second, we analyze the link from R to D_n. From (19), the received signal used for detecting $x_n[i]$ at the destination can be written as

$$y_{\mathrm{D},n}[i] = \underbrace{\sqrt{P_{\mathrm{R}}}\mathbb{E}\left\{\mathbf{g}_{\mathrm{RD},n}^T\mathbf{a}_n\right\}x_n[i-d]}_{\text{desired signal}} + \underbrace{\tilde{n}_{\mathrm{D},n}[i]}_{\text{effective noise}} \quad (26)$$

where the effective noise $\tilde{n}_{\mathrm{D},n}[i]$ is given by

$$\begin{aligned}\tilde{n}_{\mathrm{D},n}[i] &= \sqrt{P_{\mathrm{R}}}\left(\mathbf{g}_{\mathrm{RD},n}^T\mathbf{a}_n - \mathbb{E}\left\{\mathbf{g}_{\mathrm{RD},n}^T\mathbf{a}_n\right\}\right)x_n[i-d] \\ &+ \sqrt{P_{\mathrm{R}}}\sum_{j\neq n}^{N}\mathbf{g}_{\mathrm{RD},n}^T\mathbf{a}_j x_j[i-d] + \mathbf{g}_{\mathrm{RD},n}^T\mathbf{n}_3[i] \\ &+ n_{4,n}[i] + n_{\mathrm{D},n}[i]. \quad (27)\end{aligned}$$

From (24) to (27), the achievable rate for DF strategy in the full-duplex mode is

$$\mathbf{S}_{\mathrm{FD,DF}}^{\diamond} = \frac{T-\tau}{T}\sum_{n=1}^{N}\log_2\left(1+\min(\mathrm{SINR}_{\mathrm{SR},n}^{\diamond}, \mathrm{SINR}_{\mathrm{RD},n}^{\diamond})\right) \quad (28)$$

where the symbol $\diamond \in \{\mathrm{MR}, \mathrm{ZF}\}$ corresponds to MRC/MRT and ZF processing, respectively, T is the length of the coherence interval (in symbols), τ is the number of training symbols, $\mathrm{SINR}_{\mathrm{SR},n}^{\diamond}$ and $\mathrm{SINR}_{\mathrm{RD},n}^{\diamond}$ denote the average signal-to-interference-plus-noise ratio (SINR) of transmission links $S_n \to R$ and $R \to D_n$, respectively. From (24), the $\mathrm{SINR}_{\mathrm{SR},n}^{\diamond}$ is written as:

$$\mathrm{SINR}_{\mathrm{SR},n}^{\diamond} = \frac{P_{\mathrm{S}}\left|A_{\mathrm{SR},n}\right|^2}{\left(\begin{array}{l} P_{\mathrm{S}}B_{\mathrm{SR},n} + P_{\mathrm{S}}C_{\mathrm{SR},n} + D_{\mathrm{SR},n} + \\ P_{\mathrm{R}}E_{\mathrm{SR},n} + F_{\mathrm{SR},n} + G_{\mathrm{SR},n} + H_{\mathrm{SR},n}\end{array}\right)} \quad (29)$$

where

$$A_{\mathrm{SR},n} = \mathbb{E}\{\mathbf{w}_n^H\mathbf{g}_{\mathrm{SR},n}\} \quad (30)$$

$$B_{\mathrm{SR},n} = \mathbb{V}\mathrm{ar}(\mathbf{w}_n^H\mathbf{g}_{\mathrm{SR},n}) \quad (31)$$

$$C_{\mathrm{SR},n} = \sum_{j\neq n}^{N}\mathbb{E}\left\{\left|\mathbf{w}_n^H\mathbf{g}_{\mathrm{SR},j}\right|^2\right\} \quad (32)$$

$$D_{\mathrm{SR},n} = \sum_{j=1}^{N}\mathbb{E}\left\{\left|\mathbf{w}_n^H\mathbf{g}_{\mathrm{SR},j}n_{1,j}[i]\right|^2\right\} \quad (33)$$

$$E_{\mathrm{SR},n} = \mathbb{E}\left\{\left\|\mathbf{w}_n^H\mathbf{G}_{\mathrm{LI}}\mathbf{A}\right\|^2\right\} \quad (34)$$

$$F_{\mathrm{SR},n} = \mathbb{E}\left\{\left|\mathbf{w}_n^H\mathbf{G}_{\mathrm{LI}}\mathbf{n}_3[i]\right|^2\right\} \quad (35)$$

$$G_{\mathrm{SR},n} = \mathbb{E}\left\{\left|\mathbf{w}_n^H\mathbf{n}_2[i]\right|^2\right\} \quad (36)$$

$$H_{\mathrm{SR},n} = \mathbb{E}\left\{\left\|\mathbf{w}_n^H\right\|^2\right\}. \quad (37)$$

To compute $\mathrm{SINR}_{\mathrm{RD},n}^{\diamond}$, we consider (26) and obtain

$$\mathrm{SINR}_{\mathrm{RD},n}^{\diamond} = \frac{P_{\mathrm{R}}\left|A_{\mathrm{RD},n}\right|^2}{P_{\mathrm{R}}B_{\mathrm{RD},n} + P_{\mathrm{R}}C_{\mathrm{RD},n} + D_{\mathrm{RD},n} + \delta_{4,n} + 1} \quad (38)$$

where

$$A_{\mathrm{RD},n} = \mathbb{E}\left\{\mathbf{g}_{\mathrm{RD},n}^T\mathbf{a}_n\right\} \quad (39)$$

$$B_{\mathrm{RD},n} = \mathbb{V}\mathrm{ar}\left\{\mathbf{g}_{\mathrm{RD},n}^T\mathbf{a}_n\right\} \quad (40)$$

$$C_{\mathrm{RD},n} = \sum_{j\neq n}^{N}\mathbb{E}\left\{\left|\mathbf{g}_{\mathrm{RD},n}^T\mathbf{a}_j\right|^2\right\} \quad (41)$$

$$D_{\mathrm{RD},n} = \mathbb{E}\left\{\left|\mathbf{g}_{\mathrm{RD},n}^T\mathbf{n}_3[i]\right|^2\right\}. \quad (42)$$

The next two theorems provide a new exact closed-form expression of the sum spectral efficiency for MRC/MRT processing, and a new approximate closed-form expression of the sum spectral efficiency for ZF processing.

Theorem 1: Under the DF scheme and full duplex mode, the sum spectral efficiency of MRC/MRT processing is given by

$$\mathbf{S}_{\mathrm{FD,DF}}^{\mathrm{MR}} = \frac{T-\tau}{T}\sum_{n=1}^{N}\log_2\left(1+\min(\mathrm{SINR}_{\mathrm{SR},n}^{\mathrm{MR}},\mathrm{SINR}_{\mathrm{RD},n}^{\mathrm{MR}})\right) \tag{43}$$

where

$$\mathrm{SINR}_{\mathrm{SR},n}^{\mathrm{MR}} = \frac{N_{\mathrm{rx}}P_{\mathrm{S}}\beta_{\mathrm{SR},n}^2}{N_{\mathrm{rx}}P_{\mathrm{S}}A_1+P_{\mathrm{S}}A_2+P_{\mathrm{R}}A_3+A_4} \tag{44}$$

$$\mathrm{SINR}_{\mathrm{RD},n}^{\mathrm{MR}} = \frac{N_{\mathrm{tx}}P_{\mathrm{R}}\beta_{\mathrm{RD},n}^2}{N_{\mathrm{tx}}P_{\mathrm{R}}A_5+P_{\mathrm{R}}A_6+A_7} \tag{45}$$

$$A_1 = \lambda_1\beta_{\mathrm{SR},n}^2+(1+\lambda_1)\sum_{j=1}^{N}\frac{\lambda_{\mathrm{P}}\beta_{\mathrm{SR},j}^2}{\tau} \tag{46}$$

$$A_2 = (1+\lambda_1)(1+\mu_1)\sigma_{\mathrm{SR},n}^2\sum_{j=1}^{N}\beta_{\mathrm{SR},j} \tag{47}$$

$$A_3 = (1+\lambda_2)(1+\mu_1)\sigma_{\mathrm{LI}}^2\sigma_{\mathrm{SR},n}^2 \tag{48}$$

$$A_4 = (1+\mu_1)\sigma_{\mathrm{SR},n}^2 \tag{49}$$

$$A_5 = \left(\frac{(1+\mu_2)N\lambda_{\mathrm{P}}}{\tau}+\mu_2\right)\beta_{\mathrm{RD},n}^2 \tag{50}$$

$$A_6 = (1+\lambda_2)(1+\mu_2)\beta_{\mathrm{RD},n}\sum_{j=1}^{N}\sigma_{\mathrm{RD},j}^2 \tag{51}$$

$$A_7 = (1+\mu_2)\sum_{j=1}^{N}\sigma_{\mathrm{RD},j}^2. \tag{52}$$

Proof: See Appendix A.

Theorem 2: Under the DF scheme and full duplex mode, the sum spectral efficiency of ZF processing can be approximated as

$$\mathbf{S}_{\mathrm{FD,DF}}^{\mathrm{ZF}} \approx \frac{T-\tau}{T}\sum_{n=1}^{N}\log_2\left(1+\min(\mathrm{SINR}_{\mathrm{SR},n}^{\mathrm{ZF}},\mathrm{SINR}_{\mathrm{RD},n}^{\mathrm{ZF}})\right) \tag{53}$$

where

$$\mathrm{SINR}_{\mathrm{SR},n}^{\mathrm{ZF}} = \frac{P_{\mathrm{S}}\theta_{\mathrm{SR},n}^2}{P_{\mathrm{S}}B_1+P_{\mathrm{R}}B_2+B_3} \tag{54}$$

$$\mathrm{SINR}_{\mathrm{RD},n}^{\mathrm{ZF}} = \frac{P_{\mathrm{R}}\theta_{\mathrm{RD},n}^2}{P_{\mathrm{R}}B_4+B_5} \tag{55}$$

$$\begin{aligned}\xi_{\diamond,i_1i_2} &= \left(\frac{2\lambda_{\mathrm{P}}\varepsilon_{\diamond,i_1}\theta_{\diamond,i_1}^2}{(N_\diamond-N)\tau\eta_{\diamond,i_1}}+\theta_{\diamond,i_1}^2\right)\delta(i_1,i_2)\\ &+\frac{\varepsilon_{\diamond,i_1}\left(\tau+\lambda_{\mathrm{P}}\eta_{\diamond,i_2}\theta_{\diamond,i_2}^2\sum_{l=1}^{N}\eta_{\diamond,l}^{-1}\right)+\lambda_{\mathrm{P}}\theta_{\diamond,i_1}^2\sum_{l=1}^{N}\varepsilon_{\diamond,l}}{(N_\diamond-N)\tau\eta_{\diamond,i_2}}\\ &+\frac{\lambda_{\mathrm{P}}}{\tau}\left(\theta_{\diamond,i_1}^2\theta_{\diamond,i_2}^2+\frac{\varepsilon_{\diamond,i_1}^2}{(N_\diamond-N)^2\eta_{\diamond,i_2}^2}\right.\\ &\left.+\sum_{l=1}^{N}\sum_{m=1}^{N}\frac{\varepsilon_{\diamond,i_1}\varepsilon_{\diamond,m}}{(N_\diamond-N)^2\eta_{\diamond,i_2}\eta_{\diamond,l}}\right)\end{aligned} \tag{56}$$

where $\diamond \in \{\mathrm{SR},\mathrm{RD}\}$, $i_1,i_2 \in \{1,\cdots,N\}$, $N_\diamond = \begin{cases}N_{\mathrm{rx}}, & \diamond\equiv\mathrm{SR}\\ N_{\mathrm{tx}}, & \diamond\equiv\mathrm{RD}\end{cases}$ and $\delta(i_1,i_2) = \begin{cases}1, & i_1=i_2\\ 0, & i_1\neq i_2\end{cases}$.

$$B_1 = (1+\lambda_1)\sum_{j=1}^{n}\left(\xi_{\mathrm{SR},jn}+\mu_1\beta_{\mathrm{SR},j}\varphi_{\mathrm{SR},n}\right)-\theta_{\mathrm{SR},n}^2 \tag{57}$$

$$B_2 = (1+\mu_1)(1+\lambda_2)\sigma_{\mathrm{LI}}^2\varphi_{\mathrm{SR},n} \tag{58}$$

$$B_3 = (1+\mu_1)\varphi_{\mathrm{SR},n} \tag{59}$$

$$B_4 = (1+\mu_2)\left(\sum_{j=1}^{n}\xi_{\mathrm{RD},nj}+\lambda_2\beta_{\mathrm{RD},n}\sum_{j=1}^{N}\varphi_{\mathrm{RD},j}\right)-\theta_{\mathrm{RD},n}^2 \tag{60}$$

$$B_5 = (1+\mu_2)\sum_{j=1}^{N}\varphi_{\mathrm{RD},j}. \tag{61}$$

and $\theta_{\diamond,i}$, $\varphi_{\diamond,i}$ and $\xi_{\diamond,i_1i_2}$ are given in (16), (18) and (56), respectively.

Proof: See Appendix B.

For comparison, we now study an idealistic scheme in which the relay station and destinations can detect the signals based on the instantaneous CSI. With MRC/MRT and ZF processing, the achievable ergodic sum rates for DF strategy and full-duplex mode are given in (62), where "$\widetilde{\mathrm{SINR}}_{\mathrm{SR},n}^{\diamond}$" and "$\widetilde{\mathrm{SINR}}_{\mathrm{RD},n}^{\diamond}$" are expressed in (63) and (64), as shown at the top of the next page.

B. DF POWER SCALING LAWS

In general, power scaling is an important characteristic of massive MIMO systems since it indicates how the deployment of large-scale (massive) antenna arrays helps to scale down transmit power while maintaining the system target rate. Based on (43) and (53), when very large antenna arrays are deployed at the relay station, this subsection establishes various power scaling laws for MRC/MRT and ZF processing under DF strategy. To be specific, the analysis is performed in the limiting case of $N_{\mathrm{rx}}\to\infty$, $N_{\mathrm{tx}}\to\infty$, and $N_{\mathrm{rx}}=\kappa N_{\mathrm{tx}}$, $\kappa>0$. In order to understand the power scaling behaviors, define three power scaling coefficients $a\geq 0$, $b\geq 0$, and $c\geq 0$ such that $P_{\mathrm{S}}=\overline{P}_{\mathrm{S}}/N_{\mathrm{rx}}^a$, $P_{\mathrm{R}}=\overline{P}_{\mathrm{R}}/N_{\mathrm{tx}}^b$ and $P_{\mathrm{P}}=\overline{P}_{\mathrm{P}}/N_{\mathrm{rx}}^c$, where $\overline{P}_{\mathrm{S}}$, $\overline{P}_{\mathrm{R}}$ and $\overline{P}_{\mathrm{P}}$ are fixed power parameters that are independent of N_{rx} and N_{tx}.

It is easy to see that, when $c>1$, both $\mathbf{S}_{\mathrm{FD,DF}}^{\mathrm{MR}}$ and $\mathbf{S}_{\mathrm{FD,DF}}^{\mathrm{ZF}}$ tend to zero, while they converge to a constant when $c\leq 1$. Furthermore, the following corollaries give the values of $\mathbf{S}_{\mathrm{FD,DF}}^{\mathrm{MR}}$ and $\mathbf{S}_{\mathrm{FD,DF}}^{\mathrm{ZF}}$ for various cases concerning a, b and c.

$$\tilde{\mathbf{S}}_{\mathrm{FD,DF}}^{\diamond} = \frac{T-\tau}{T}\sum_{n=1}^{N}\mathbb{E}\left\{\log_2\left(1+\min(\widetilde{\mathrm{SINR}}_{\mathrm{SR},n}^{\diamond}, \widetilde{\mathrm{SINR}}_{\mathrm{RD},n}^{\diamond})\right)\right\} \tag{62}$$

where

$$\widetilde{\mathrm{SINR}}_{\mathrm{SR},n}^{\diamond} = \frac{P_{\mathrm{S}}\left|\mathbf{w}_n^H\mathbf{g}_{\mathrm{SR},n}\right|^2}{P_{\mathrm{S}}\sum\limits_{j\neq n}^{N}\left|\mathbf{w}_n^H\mathbf{g}_{\mathrm{SR},j}\right|^2+\sum\limits_{j=1}^{N}\left|\mathbf{w}_n^H\mathbf{g}_{\mathrm{SR},j}n_{1,j}[i]\right|^2+P_{\mathrm{R}}\left\|\mathbf{w}_n^H\mathbf{G}_{\mathrm{LI}}\mathbf{A}\right\|^2+\left|\mathbf{w}_n^H\mathbf{G}_{\mathrm{LI}}\mathbf{n}_3[i]\right|^2+\left|\mathbf{w}_n^H\mathbf{n}_2[i]\right|^2+\left\|\mathbf{w}_n^H\right\|^2} \tag{63}$$

$$\widetilde{\mathrm{SINR}}_{\mathrm{RD},n}^{\diamond} = \frac{P_{\mathrm{R}}\left|\mathbf{g}_{\mathrm{RD},n}^T\mathbf{a}_n\right|^2}{P_{\mathrm{R}}\sum\limits_{j\neq n}^{N}\left|\mathbf{g}_{\mathrm{RD},n}^T\mathbf{a}_j\right|^2+\left|\mathbf{g}_{\mathrm{RD},n}^T\mathbf{n}_3[i]\right|^2+\delta_{4,n}+1} \tag{64}$$

1) DF POWER SCALING LAWS WITH MRC/MRT PROCESSING

Corollary 1: When $a+c<1$ and $b+c<1$, the sum spectral efficiency of MRC/MRT processing in (43) can be expressed as follows:

$$\mathbf{S}_{\mathrm{FD,DF}}^{\mathrm{MR}} \to \frac{T-\tau}{T}\sum_{n=1}^{N}\log_2\left(1+\min\left(\frac{\beta_{\mathrm{SR},n}^2}{A_1},\frac{1}{A_8}\right)\right) \tag{65}$$

where

$$A_8 = \frac{(1+\mu_2)N\lambda_{\mathrm{P}}}{\tau}+\mu_2. \tag{66}$$

The expression in (65) shows that, when both N_{rx} and N_{tx} tend to infinity, the rate performance can still be maintained when scaling down the transmit powers of sources, relay and pilots proportionally to $1/N_{\mathrm{rx}}^a$, $1/N_{\mathrm{tx}}^b$ and $1/N_{\mathrm{rx}}^c$, respectively. Furthermore, the absence of parameters λ_2, μ_1, μ_{P} and σ_{LI}^2 from (65) indicates that the rate performance for MRC/MRT processing in the DF scheme is not affected by the loop interference and relay's hardware impairments in the limiting case considered. The hardware impairments of sources and destinations, represented by parameters λ_1, λ_{P} and μ_2 are the only factors that limit the system performance.

Corollary 2: When $a=1$, $b=0$ and $c=0$, the sum spectral efficiency of MRC/MRT processing in (43) can be expressed as

$$\mathbf{S}_{\mathrm{FD,DF}}^{\mathrm{MR}} \to \frac{T-\tau}{T}\sum_{n=1}^{N} \times\log_2\left(1+\min\left(\frac{\overline{P}_{\mathrm{S}}\beta_{\mathrm{SR},n}^2}{\overline{P}_{\mathrm{S}}A_1+\overline{P}_{\mathrm{R}}A_3+A_4},\frac{1}{A_8}\right)\right). \tag{67}$$

Corollary 3: When $a=1$, $0<b<1$ and $c=0$, the sum spectral efficiency of MRC/MRT processing in (43) can be expressed as

$$\mathbf{S}_{\mathrm{FD,DF}}^{\mathrm{MR}} \to \frac{T-\tau}{T}\sum_{n=1}^{N}\log_2\left(1+\min\left(\frac{\overline{P}_{\mathrm{S}}\beta_{\mathrm{SR},n}^2}{\overline{P}_{\mathrm{S}}A_1+A_4},\frac{1}{A_8}\right)\right). \tag{68}$$

Observe that the sum spectral efficiency in Corollary 3 is greater than that in Corollary 2. This means that power scaling in the relay's transmitter ($b>0$) not only can save energy but also improve the system's rate performance. This phenomenon can be explained as follows. As the number of relay's antennas increases, the power of the relay's transmitter decreases and the impact of loop interference experienced by the relay's receiver decreases. This results in better communication performance at the relay's receiver without affecting the communication performance of the destination. Therefore, the performance of the whole system should improve.

Corollary 4: When $a<1$, $b=1$ and $c=0$, the sum spectral efficiency of MRC/MRT processing in (43) can be expressed as

$$\mathbf{S}_{\mathrm{FD,DF}}^{\mathrm{MR}} \to \frac{T-\tau}{T}\sum_{n=1}^{N}\log_2\left(1+\min\left(\frac{\beta_{\mathrm{SR},n}^2}{A_1},\frac{\overline{P}_{\mathrm{R}}\beta_{\mathrm{RD},n}^2}{\overline{P}_{\mathrm{R}}A_5+A_7}\right)\right). \tag{69}$$

Corollary 5: When $a=1$, $b=1$ and $c=0$, the sum spectral efficiency of MRC/MRT processing in (43) can be expressed as

$$\mathbf{S}_{\mathrm{FD,DF}}^{\mathrm{MR}} \to \frac{T-\tau}{T}\sum_{n=1}^{N}\log_2 \times\left(1+\min\left(\frac{\overline{P}_{\mathrm{S}}\beta_{\mathrm{SR},n}^2}{\overline{P}_{\mathrm{S}}A_1+A_4},\frac{\overline{P}_{\mathrm{R}}\beta_{\mathrm{RD},n}^2}{\overline{P}_{\mathrm{R}}A_5+A_7}\right)\right). \tag{70}$$

Corollary 4 and Corollary 5 thus reveal the effect of transmit power of the sources on system performance under MRC/MRT processing. It is observed that the sum spectral efficiency stated in Corollary 4 is greater than that in Corollary 5.

Corollary 6: When $a+c=1$, $b=0$ and $0<c<1$ (which implies that $0<a<1$), the sum spectral efficiency

of MRC/MRT processing in (43) can be expressed as follows

$$\mathbf{S}_{\mathrm{FD,DF}}^{\mathrm{MR}} \to \frac{T-\tau}{T}\sum_{n=1}^{N}\log_2 \times\left(1+\min\left(\frac{\overline{P}_{\mathrm{S}}\beta_{\mathrm{SR},n}^2}{\overline{P}_{\mathrm{S}}A_1+\overline{P}_{\mathrm{R}}A_9+A_{10}},\frac{1}{A_8}\right)\right) \tag{71}$$

where

$$A_9 = \frac{(1+\lambda_2)(1+\mu_1)(1+\mu_{\mathrm{P}})\sigma_{\mathrm{LI}}^2}{\tau\overline{P}_{\mathrm{P}}} \tag{72}$$

$$A_{10} = \frac{(1+\mu_1)(1+\mu_{\mathrm{P}})}{\tau\overline{P}_{\mathrm{P}}}. \tag{73}$$

Corollary 7: When $a+c=1$, $b+c<1$, $a,b,c>0$ (or equivalently $a+c=1$ and $0<b<a<1$), the sum spectral efficiency of MRC/MRT processing in (43) can be expressed as

$$\mathbf{S}_{\mathrm{FD,DF}}^{\mathrm{MR}} \to \frac{T-\tau}{T}\sum_{n=1}^{N}\log_2\left(1+\min\left(\frac{\overline{P}_{\mathrm{S}}\beta_{\mathrm{SR},n}^2}{\overline{P}_{\mathrm{S}}A_1+A_{10}},\frac{1}{A_8}\right)\right). \tag{74}$$

It is observed that the sum spectral efficiency stated in Corollary 7 is greater than that in Corollary 6. This observation reveals that, similar to Corollary 2 and Corollary 3, power scaling in the relay's transmitter ($b>0$) helps to save energy and improve the system performance.

Corollary 8: When $a+c<1$, $b+c=1$ and $c>0$, the sum spectral efficiency of MRC/MRT processing in (43) can be expressed as

$$\mathbf{S}_{\mathrm{FD,DF}}^{\mathrm{MR}} \to \frac{T-\tau}{T}\sum_{n=1}^{N}\log_2\left(1+\min\left(\frac{\beta_{\mathrm{SR},n}^2}{A_1},\frac{\overline{P}_{\mathrm{R}}\beta_{\mathrm{RD},n}^2}{\overline{P}_{\mathrm{R}}A_5+A_{11}}\right)\right) \tag{75}$$

where

$$A_{11} = \frac{(1+\mu_{\mathrm{P}})(1+\mu_2)N\kappa^c}{\tau\overline{P}_{\mathrm{P}}}. \tag{76}$$

Corollary 9: When $a+c=1$, $b+c=1$ and $0<c<1$, the sum spectral efficiency of MRC/MRT processing in (43) can be expressed as

$$\mathbf{S}_{\mathrm{FD,DF}}^{\mathrm{MR}} \to \frac{T-\tau}{T}\sum_{n=1}^{N} \times\log_2\left(1+\min\left(\frac{\overline{P}_{\mathrm{S}}\beta_{\mathrm{SR},n}^2}{\overline{P}_{\mathrm{S}}A_1+A_{10}},\frac{\overline{P}_{\mathrm{R}}\beta_{\mathrm{RD},n}^2}{\overline{P}_{\mathrm{R}}A_5+A_{11}}\right)\right). \tag{77}$$

By comparing Corollary 8 and Corollary 9, we can see that, the hardware impairment of the relay's receiver will affect the system performance when $a+c=1$, but not when $a+c<1$. It is pointed out that the conditions in Corollary 9 imply that $0<a<1$ and $0<b<1$. When $a=b=c=0.5$, compared to the case of ideal hardware in [17], it is seen that the sum spectral efficiency of MRC/MRT processing is affected by hardware impairments from the sources, relay's receiver and destinations.

Corollary 10: When $a=0$, $b=0$ and $c=1$, the sum spectral efficiency of MRC/MRT processing in (43) can be expressed as

$$\mathbf{S}_{\mathrm{FD,DF}}^{\mathrm{MR}} \to \frac{T-\tau}{T}\sum_{n=1}^{N}\log_2 \times\left(1+\min\left(\frac{\overline{P}_{\mathrm{S}}\beta_{\mathrm{SR},n}^2}{\overline{P}_{\mathrm{S}}A_{12}+\overline{P}_{\mathrm{R}}A_{13}+A_{10}},\frac{\overline{P}_{\mathrm{R}}\beta_{\mathrm{RD},n}^2}{\overline{P}_{\mathrm{R}}A_{14}+A_{11}}\right)\right) \tag{78}$$

where

$$A_{12} = A_1+(1+\lambda_1)A_{10}\sum_{j=1}^{N}\beta_{\mathrm{SR},j} \tag{79}$$

$$A_{13} = (1+\lambda_2)\sigma_{\mathrm{LI}}^2 A_{10} \tag{80}$$

$$A_{14} = A_5+(1+\lambda_2)\beta_{\mathrm{RD},n}A_{11}. \tag{81}$$

In summary, with MRC/MRT processing and DF strategy, Corollary 1 to Corollary 10 show that, as the sizes of antenna arrays tend to infinity, one can scale down the transmitted powers of sources, relay station and pilots proportionally to various power scaling coefficients ($a,b,c\geq 0$, $a+c\leq 1$ and $b+c\leq 1$), while maintaining a given system performance. The rate expressions in all these corollaries indicate that, whenever $b>0$, the impact of loop interference can be eliminated. This favorable result is consistent with the fact that when the transmit power of the relay station is reduced, the level of the loop interference also declines.

2) DF POWER SCALING LAWS WITH ZF PROCESSING

Corollary 11: When $0\leq a,b<1$ and $c=0$, the sum spectral efficiency of ZF processing in (53) can be expressed as

$$\mathbf{S}_{\mathrm{FD,DF}}^{\mathrm{ZF}} \to \frac{T-\tau}{T}\sum_{n=1}^{N}\log_2\left(1+\min\left(\frac{1}{B_6},\frac{1}{B_7}\right)\right) \tag{82}$$

where

$$B_6 = \frac{\lambda_{\mathrm{P}}(1+\lambda_1)\sum_{j=1}^{N}\theta_{\mathrm{SR},j}^2+\tau\lambda_1}{\tau} \tag{83}$$

$$B_7 = \frac{\lambda_{\mathrm{P}}(1+\mu_2)\sum_{j=1}^{N}\theta_{\mathrm{RD},j}^2+\tau\mu_2}{\tau}. \tag{84}$$

Corollary 12: When $a+c<1$, $b+c<1$, $0\leq a,b<1$ and $0<c<1$, the sum spectral efficiency of ZF processing in (53) can be expressed as

$$\mathbf{S}_{\mathrm{FD,DF}}^{\mathrm{ZF}} \to \frac{T-\tau}{T}\sum_{n=1}^{N}\log_2\left(1+\min\left(\frac{1}{\lambda_1},\frac{1}{\mu_2}\right)\right). \tag{85}$$

With ZF processing and DF strategy, Corollary 11 and Corollary 12 reveal the effect of pilot power on system performance. Different from the case of MRC/MRT processing, when $a+c<1$, $b+c<1$ and $0<c<1$, the effect of hardware impairment of λ_{P} and μ_{P} can be eliminated, and $\mathbf{S}_{\mathrm{FD,DF}}^{\mathrm{ZF}} \geq \mathbf{S}_{\mathrm{FD,DF}}^{\mathrm{MR}}$ in the power scaling case of $a+c<1$, $b+c<1$, $0 \leq a,b<1$ and $0<c<1$. This indicates that the hardware impairments of sources and destinations, represented by parameters λ_1 and μ_2 are the only factors that limit the system performance in this power scaling law.

Corollary 13: When $a=1$, $b=0$ and $c=0$, the sum spectral efficiency of ZF processing in (53) can be expressed as

$$\mathbf{S}_{\mathrm{FD,DF}}^{\mathrm{ZF}} \to \frac{T-\tau}{T}\sum_{n=1}^{N}\log_2 \times\left(1+\min\left(\frac{\bar{P}_{\mathrm{S}}}{\bar{P}_{\mathrm{S}}B_6+\bar{P}_{\mathrm{R}}B_8B_9+B_9B_{10}},\frac{1}{B_7}\right)\right) \tag{86}$$

where

$$B_8=(1+\mu_1)(1+\lambda_2)\sigma_{\mathrm{LI}}^2 \tag{87}$$

$$B_9=\frac{\eta_{\mathrm{SR},n}}{\beta_{\mathrm{SR},n}^2}+\frac{\lambda_{\mathrm{P}}}{\tau}\sum_{j=1}^{N}\eta_{\mathrm{SR},j}^{-1} \tag{88}$$

$$B_{10}=1+\mu_1. \tag{89}$$

Corollary 14: When $a=1$, $0<b<1$ and $c=0$, the sum spectral efficiency of ZF processing in (53) can be expressed as

$$\mathbf{S}_{\mathrm{FD,DF}}^{\mathrm{ZF}} \to \frac{T-\tau}{T}\sum_{n=1}^{N}\log_2\left(1+\min\left(\frac{\bar{P}_{\mathrm{S}}}{\bar{P}_{\mathrm{S}}B_6+B_9B_{10}},\frac{1}{B_7}\right)\right). \tag{90}$$

Observe that the sum spectral efficiency in Corollary 14 is greater than that in Corollary 13 for ZF processing and DF strategy. This is because as the number of relay's antennas increases, decreasing the loop interference has a much stronger effect on the system performance, compared with decreasing the relay's transmit power.

Corollary 15: When $a<1$, $b=1$ and $c=0$, the sum spectral efficiency of ZF processing in (53) can be expressed as

$$\mathbf{S}_{\mathrm{FD,DF}}^{\mathrm{ZF}} \to \frac{T-\tau}{T}\sum_{n=1}^{N}\log_2\left(1+\min\left(\frac{1}{B_6},\frac{\bar{P}_{\mathrm{R}}\theta_{\mathrm{RD},n}^2}{\bar{P}_{\mathrm{R}}B_7\theta_{\mathrm{RD},n}^2+B_{11}}\right)\right) \tag{91}$$

where

$$B_{11}=(1+\mu_2)\sum_{j=1}^{n}\left(\eta_{\mathrm{RD},j}^{-1}+\frac{\lambda_{\mathrm{P}}}{\tau}\theta_{\mathrm{RD},j}^2\sum_{l=1}^{N}\eta_{\mathrm{RD},l}^{-1}\right). \tag{92}$$

Corollary 16: When $a=1$, $b=1$ and $c=0$, the sum spectral efficiency of ZF processing in (53) can be expressed as

$$\mathbf{S}_{\mathrm{FD,DF}}^{\mathrm{ZF}} \to \frac{T-\tau}{T}\sum_{n=1}^{N}\log_2 \times\left(1+\min\left(\frac{\bar{P}_{\mathrm{S}}}{\bar{P}_{\mathrm{S}}B_6+B_9B_{10}},\frac{\bar{P}_{\mathrm{R}}\theta_{\mathrm{RD},n}^2}{\bar{P}_{\mathrm{R}}B_7\theta_{\mathrm{RD},n}^2+B_{11}}\right)\right). \tag{93}$$

Similar to the results of MRC/MRT processing, Corollary 15 and Corollary 16 show that, when $a=1$, the hardware impairment of the relay's receiver will reduce the rate performance achieved with ZF processing and DF strategy.

Corollary 17: When $a+c=1$, $b=0$ and $0<c<1$ (which implies that $0<a<1$), the sum spectral efficiency of ZF processing in (53) can be expressed as

$$\mathbf{S}_{\mathrm{FD,DF}}^{\mathrm{ZF}} \to \frac{T-\tau}{T}\sum_{n=1}^{N}\log_2 \times\left(1+\min\left(\frac{\bar{P}_{\mathrm{S}}\beta_{\mathrm{SR},n}^2B_{12}}{\bar{P}_{\mathrm{S}}B_{13}+\bar{P}_{\mathrm{R}}B_8+B_{10}},\frac{1}{\mu_2}\right)\right) \tag{94}$$

where

$$B_{12}=\frac{\tau\bar{P}_{\mathrm{P}}}{1+\mu_{\mathrm{P}}} \tag{95}$$

$$B_{13}=\lambda_1\beta_{\mathrm{SR},n}^2B_{12}. \tag{96}$$

Corollary 18: When $a+c=1$, $b+c<1$, $a,b,c>0$ (or equivalently $a+c=1$ and $0<b<a<1$), the sum spectral efficiency of ZF processing in (53) can be expressed as

$$\mathbf{S}_{\mathrm{FD,DF}}^{\mathrm{ZF}} \to \frac{T-\tau}{T}\sum_{n=1}^{N}\log_2\left(1+\min\left(\frac{\bar{P}_{\mathrm{S}}\beta_{\mathrm{SR},n}^2B_{12}}{\bar{P}_{\mathrm{S}}B_{13}+B_{10}},\frac{1}{\mu_2}\right)\right). \tag{97}$$

The results of Corollary 17 and Corollary 18 once again show that, compared with reducing the power at the relay's transmitter, reducing the loop interference can improve system performance for ZF processing and DF strategy.

Corollary 19: When $a+c<1$, $b+c=1$ and $c>0$, the sum spectral efficiency of ZF processing in (53) can be expressed as

$$\mathbf{S}_{\mathrm{FD,DF}}^{\mathrm{ZF}} \to \frac{T-\tau}{T}\sum_{n=1}^{N}\log_2\left(1+\min\left(\frac{1}{\lambda_1},\frac{\bar{P}_{\mathrm{R}}\beta_{\mathrm{RD},n}^2B_{12}}{\bar{P}_{\mathrm{R}}B_{14}+B_{15}}\right)\right) \tag{98}$$

where

$$B_{14}=\mu_2\beta_{\mathrm{RD},n}^2B_{12} \tag{99}$$

$$B_{15}=(1+\mu_2)N\kappa^c. \tag{100}$$

Comparing Corollary 8 and Corollary 19 has $\mathbf{S}_{\mathrm{FD,DF}}^{\mathrm{ZF}} \geq \mathbf{S}_{\mathrm{FD,DF}}^{\mathrm{MR}}$ in this power scaling case. This shows that ZF processing can have better rate performance than MRC/MRT processing under DF strategy.

Corollary 20: When $a+c=1$, $b+c=1$ and $0<c<1$, the sum spectral efficiency of ZF processing in (53) can be expressed as

$$\mathbf{S}_{\mathrm{FD,DF}}^{\mathrm{ZF}} \to \frac{T-\tau}{T}\sum_{n=1}^{N}\log_2 \times\left(1+\min\left(\frac{\bar{P}_{\mathrm{S}}\beta_{\mathrm{SR},n}^2 B_{12}}{\bar{P}_{\mathrm{S}}B_{13}+B_{10}},\frac{\bar{P}_{\mathrm{R}}\beta_{\mathrm{RD},n}^2 B_{12}}{\bar{P}_{\mathrm{R}}B_{14}+B_{15}}\right)\right). \tag{101}$$

The conditions in Corollary 20 imply that $0<a<1$ and $0<b<1$. When $a=b=c=0.5$, compared to the case of ideal hardware in [17], similar to MRC/MRT processing, the sum spectral efficiency of ZF processing is also affected by hardware impairments from the source, relay's receiver and destinations.

Corollary 21: When $a=0$, $b=0$ and $c=1$, the sum spectral efficiency of ZF processing in (53) can be expressed as

$$\mathbf{S}_{\mathrm{FD,DF}}^{\mathrm{ZF}} \to \frac{T-\tau}{T}\sum_{n=1}^{N}\log_2\left(1+\min\left(\frac{\bar{P}_{\mathrm{S}}\beta_{\mathrm{SR},n}^2 B_{12}}{\bar{P}_{\mathrm{S}}B_{16}+\bar{P}_{\mathrm{R}}B_8+B_{10}},\frac{\bar{P}_{\mathrm{R}}\beta_{\mathrm{RD},n}^2 B_{12}}{\bar{P}_{\mathrm{R}}B_{17}+B_{15}}\right)\right) \tag{102}$$

where

$$B_{16}=B_{13}+(1+\lambda_1)(1+\mu_1)\sum_{j=1}^{N}\beta_{\mathrm{SR},j} \tag{103}$$

$$B_{17}=B_{14}+(1+\lambda_2)(1+\mu_2)N\beta_{\mathrm{RD},n}\kappa^c. \tag{104}$$

Comparing Corollary 10 and Corollary 21 has $\mathbf{S}_{\mathrm{FD,DF}}^{\mathrm{ZF}} \geq \mathbf{S}_{\mathrm{FD,DF}}^{\mathrm{MR}}$ in this power scaling case. This once again reveals that the rate performance of ZF processing is better than that of MRC/MRT processing in DF strategy.

With ZF processing and DF strategy, Corollary 11 to Corollary 21 show that, as the sizes of antenna arrays at the relay tend to infinity, the transmitted powers of sources, relay station and pilots can be scaled down proportionally to different coefficients ($a, b, c \geq 0$, $a+c \leq 1$ and $b+c \leq 1$), while maintaining a given system performance. The rate expressions in all these corollaries indicate that, whenever $b>0$, the impact of loop interference can be eliminated and the system's rate performance can be improved. Furthermore, when $a+c<1$, $b+c<1$, $0 \leq a, b<1$ and $0<c<1$, the hardware impairments of λ_{P} and μ_{P} in sources, relay and destinations can be eliminated for ZF processing and DF strategy.

C. DF HALF-DUPLEX SCENARIO

For comparison, the sum spectral efficiencies of the half-duplex mode with MRC/MRT and ZF processing can be obtained directly from (43) and (53) by neglecting the loop interference, imposing a pre-log factor of 1/2 and doubling the transmit powers [17]. The results are summarized in Corollary 22 and Corollary 23.

Corollary 22: The sum spectral efficiency of the half-duplex DF relaying with MRC/MRT processing is given by

$$\mathbf{S}_{\mathrm{HD,DF}}^{\mathrm{MR}}=\frac{T-\tau}{2T}\sum_{n=1}^{N}\log_2\left(1+\min\left(\frac{2N_{\mathrm{rx}}P_{\mathrm{S}}\beta_{\mathrm{SR},n}^2}{2N_{\mathrm{rx}}P_{\mathrm{S}}A_1+2P_{\mathrm{S}}A_2+A_4},\frac{2N_{\mathrm{tx}}P_{\mathrm{R}}\beta_{\mathrm{RD},n}^2}{2N_{\mathrm{tx}}P_{\mathrm{R}}A_5+2P_{\mathrm{R}}A_6+A_7}\right)\right). \tag{105}$$

Corollary 23: The sum spectral efficiency of the half-duplex DF relaying with ZF processing is given by

$$\mathbf{S}_{\mathrm{HD,DF}}^{\mathrm{ZF}}=\frac{T-\tau}{2T}\sum_{n=1}^{N}\times\log_2\left(1+\min\left(\frac{2P_{\mathrm{S}}\theta_{\mathrm{SR},n}^2}{2P_{\mathrm{S}}B_1+B_3},\frac{2P_{\mathrm{R}}\theta_{\mathrm{RD},n}^2}{2P_{\mathrm{R}}B_4+B_5}\right)\right). \tag{106}$$

Based on (105) and (106), one can easily obtain power scaling characteristics for the half-duplex DF relaying systems. Due to space limitation, such analysis is not included in this paper.

IV. ACHIEVABLE RATE ANALYSIS AND POWER SCALING LAWS WITH THE AF PROTOCOL

A. AF ACHIEVABLE RATE ANALYSIS

Consider the nth link $S_n \to R \to D_n$. It follows from (22) that the received signal at D_n can be rewritten as a sum of the desired signal and an effective noise term. By the same reasoning as in the case of DF strategy, the sum spectral efficiency of the AF scheme for MRC/MRT and ZF processing is lower bounded as follows [40]:

$$\mathbf{S}_{\mathrm{FD,AF}}^{\diamondsuit}=\frac{T-\tau}{T}\sum_{n=1}^{N}\log_2\left(1+\mathrm{SINR}_n^{\diamondsuit}\right) \tag{107}$$

where $\diamondsuit \in \{\mathrm{MR}, \mathrm{ZF}\}$ corresponds to MRC/MRT and ZF processing, respectively, T is the length of the coherence interval (in symbols). The $\mathrm{SINR}_n^{\diamondsuit}$ of transmission link $S_n \to R \to D_n$ is given as

$$\mathrm{SINR}_n^{\diamondsuit}=\frac{\rho^2 P_{\mathrm{S}}P_{\mathrm{R}}\left|E_{1,n}\right|^2}{\left(\begin{array}{l}\rho^2 P_{\mathrm{S}}P_{\mathrm{R}}E_{2,n}+\rho^2 P_{\mathrm{S}}P_{\mathrm{R}}E_{3,n}+\rho^2 P_{\mathrm{R}}E_{4,n}\\ +\rho^2 P_{\mathrm{R}}^2 E_{5,n}+\rho^2 P_{\mathrm{R}}E_{6,n}+\rho^2 P_{\mathrm{R}}E_{7,n}\\ +\rho^2 P_{\mathrm{R}}E_{8,n}+E_{9,n}+\delta_{4,n}+1\end{array}\right)} \tag{108}$$

where

$$E_{1,n}=\mathbb{E}\left\{\mathbf{g}_{\mathrm{RD},n}^T\mathbf{F}\mathbf{g}_{\mathrm{SR},n}\right\} \tag{109}$$

$$E_{2,n}=\mathbb{V}\mathrm{ar}\left\{\mathbf{g}_{\mathrm{RD},n}^T\mathbf{F}\mathbf{g}_{\mathrm{SR},n}\right\} \tag{110}$$

$$E_{3,n}=\sum_{j\neq n}^{N}\mathbb{E}\left\{\left|\mathbf{g}_{\mathrm{RD},n}^T\mathbf{F}\mathbf{g}_{\mathrm{SR},j}\right|^2\right\} \tag{111}$$

$$E_{4,n} = \mathbb{E}\left\{\left|\mathbf{g}_{\mathrm{RD},n}^{T}\mathbf{F}\mathbf{G}_{\mathrm{SR}}\mathbf{n}_1\left[i-1\right]\right|^2\right\} \tag{112}$$

$$E_{5,n} = \mathbb{E}\left\{\left|\mathbf{g}_{\mathrm{RD},n}^{T}\mathbf{F}\mathbf{G}_{\mathrm{LI}}\tilde{\mathbf{y}}_{\mathrm{RT}}[i-1]\right|^2\right\} \tag{113}$$

$$E_{6,n} = \mathbb{E}\left\{\left|\mathbf{g}_{\mathrm{RD},n}^{T}\mathbf{F}\mathbf{G}_{\mathrm{LI}}\mathbf{n}_3\left[i-1\right]\right|^2\right\} \tag{114}$$

$$E_{7,n} = \mathbb{E}\left\{\left|\mathbf{g}_{\mathrm{RD},n}^{T}\mathbf{F}\mathbf{n}_{\mathrm{R}}\left[i-1\right]\right|^2\right\} \tag{115}$$

$$E_{8,n} = \mathbb{E}\left\{\left|\mathbf{g}_{\mathrm{RD},n}^{T}\mathbf{F}\mathbf{n}_2\left[i-1\right]\right|^2\right\} \tag{116}$$

$$E_{9,n} = \mathbb{E}\left\{\left|\mathbf{g}_{\mathrm{RD},n}^{T}\mathbf{n}_3[i]\right|^2\right\}. \tag{117}$$

Based on (107), the following theorems establish closed-form expressions of the sum spectral efficiency with AF scheme for MRC/MRT and ZF processing.

Theorem 3: Under the AF scheme and full-duplex mode, the sum spectral efficiency of MRC/MRT processing is given by

$$\mathbf{S}_{\mathrm{FD,AF}}^{\mathrm{MR}} = \frac{T-\tau}{T}\sum_{n=1}^{N}\log_2\left(1+\mathrm{SINR}_n^{\mathrm{MR}}\right) \tag{118}$$

where

$$\mathrm{SINR}_n^{\mathrm{MR}} = \frac{P_{\mathrm{R}}P_{\mathrm{S}}E_4}{P_{\mathrm{R}}^2E_7 + P_{\mathrm{R}}P_{\mathrm{S}}E_8 + P_{\mathrm{R}}E_9 + P_{\mathrm{S}}E_{10} + E_{11}}, \tag{119}$$

$$\vartheta_{\mathrm{RD},i_1i_2} = \beta_{\mathrm{RD},i_1}\sigma_{\mathrm{RD},i_2}^2 + \left(\frac{\lambda_{\mathrm{P}}}{\tau} + \delta\left(i_1,i_2\right)\right)N_{\mathrm{tx}}\beta_{\mathrm{RD},i_1}^2 \tag{120}$$

$$\vartheta_{\mathrm{SR},i_1i_2} = \beta_{\mathrm{SR},i_1}\sigma_{\mathrm{SR},i_2}^2 + \left(\frac{\lambda_{\mathrm{P}}}{\tau} + \delta\left(i_1,i_2\right)\right)N_{\mathrm{rx}}\beta_{\mathrm{SR},i_1}^2 \tag{121}$$

where $i_1, i_2 \in \{1,\cdots,N\}$ and $\delta\left(i_1,i_2\right) = \begin{cases}1, & i_1 = i_2\\ 0, & i_1 \neq i_2\end{cases}$.

$$E_1 = \sum_{i=1}^{N}\sigma_{\mathrm{RD},i}^2\sigma_{\mathrm{SR},i}^2 \tag{122}$$

$$E_2 = \sum_{i=1}^{N}\vartheta_{\mathrm{RD},ni}\sigma_{\mathrm{SR},i}^2 \tag{123}$$

$$E_3 = \sum_{i=1}^{N}\vartheta_{\mathrm{SR},ni}\sigma_{\mathrm{RD},i}^2 \tag{124}$$

$$E_4 = N_{\mathrm{tx}}N_{\mathrm{rx}}\beta_{\mathrm{RD},n}^2\beta_{\mathrm{SR},n}^2 \tag{125}$$

$$E_5 = \sum_{i=1}^{N}\vartheta_{\mathrm{RD},ni}\vartheta_{\mathrm{SR},ni} \tag{126}$$

$$E_6 = \sum_{i=1}^{N}\vartheta_{\mathrm{RD},ni}\vartheta_{\mathrm{SR},ji} \tag{127}$$

$$E_7 = \left(\lambda_2\beta_{\mathrm{RD},n}E_1 + E_2\right)\left(1+\lambda_2\right)\left(1+\mu_1\right)\left(1+\mu_2\right)\sigma_{\mathrm{LI}}^2 \tag{128}$$

$$E_8 = \left(1+\lambda_1\right)\left(1+\mu_2\right)\left(E_5 + \sum_{j\neq n}^{N}E_6 + \mu_1E_2\sum_{j=1}^{N}\beta_{\mathrm{SR},j} + \lambda_2\beta_{\mathrm{RD},n}\sum_{n=1}^{N}E_3 + \lambda_2\mu_1\beta_{\mathrm{RD},n}E_1\sum_{j=1}^{N}\beta_{\mathrm{SR},j}\right) - E_4 \tag{129}$$

$$E_9 = \left(1+\mu_1\right)\left(1+\mu_2\right) \times\left(\left(1+\lambda_2\right)\sigma_{\mathrm{LI}}^2E_1 + \lambda_2\beta_{\mathrm{RD},n}E_1 + E_2\right) \tag{130}$$

$$E_{10} = \left(1+\lambda_1\right)\left(1+\mu_2\right)\left(\sum_{n=1}^{N}E_3 + \mu_1E_1\sum_{j=1}^{N}\beta_{\mathrm{SR},j}\right) \tag{131}$$

$$E_{11} = \left(1+\mu_1\right)\left(1+\mu_2\right)E_1. \tag{132}$$

Proof: See Appendix C.

Theorem 4: Under the AF scheme and full-duplex mode, the sum spectral efficiency of ZF processing can be approximated as

$$\mathbf{S}_{\mathrm{FD,AF}}^{\mathrm{ZF}} = \frac{T-\tau}{T}\sum_{n=1}^{N}\log_2\left(1+\mathrm{SINR}_n^{\mathrm{ZF}}\right) \tag{133}$$

$$\mathrm{SINR}_n^{\mathrm{ZF}} = \frac{P_{\mathrm{R}}P_{\mathrm{S}}F_4}{P_{\mathrm{R}}^2F_7 + P_{\mathrm{R}}P_{\mathrm{S}}F_8 + P_{\mathrm{R}}F_9 + P_{\mathrm{S}}F_{10} + F_{11}}, \tag{134}$$

$$F_1 = \sum_{i=1}^{N}\varphi_{\mathrm{RD},i}\varphi_{\mathrm{SR},i} \tag{135}$$

$$F_2 = \sum_{i=1}^{N}\xi_{\mathrm{RD},ni}\varphi_{\mathrm{SR},i} \tag{136}$$

$$F_3 = \sum_{i=1}^{N}\xi_{\mathrm{SR},ni}\varphi_{\mathrm{RD},i} \tag{137}$$

$$F_4 = \theta_{\mathrm{RD},n}^2\theta_{\mathrm{SR},n}^2 \tag{138}$$

$$F_5 = \sum_{i=1}^{N}\xi_{\mathrm{RD},ni}\xi_{\mathrm{SR},ni} \tag{139}$$

$$F_6 = \sum_{i=1}^{N}\xi_{\mathrm{RD},ni}\xi_{\mathrm{SR},ji} \tag{140}$$

$$F_7 = \left(\lambda_2\beta_{\mathrm{RD},n}F_1 + F_2\right)\left(1+\lambda_2\right)\left(1+\mu_1\right)\left(1+\mu_2\right)\sigma_{\mathrm{LI}}^2 \tag{141}$$

$$F_8 = \left(1+\lambda_1\right)\left(1+\mu_2\right)\left(F_5 + \sum_{j\neq n}^{N}F_6 + \mu_1F_2\sum_{j=1}^{N}\beta_{\mathrm{SR},j} + \lambda_2\beta_{\mathrm{RD},n}\sum_{n=1}^{N}F_3 + \lambda_2\mu_1\beta_{\mathrm{RD},n}F_1\sum_{j=1}^{N}\beta_{\mathrm{SR},j}\right) - F_4 \tag{142}$$

$$F_9 = \left(1+\mu_1\right)\left(1+\mu_2\right) \times\left(\left(1+\lambda_2\right)\sigma_{\mathrm{LI}}^2F_1 + \lambda_2\beta_{\mathrm{RD},n}F_1 + F_2\right) \tag{143}$$

$$F_{10} = (1+\lambda_1)(1+\mu_2)\left(\sum_{n=1}^{N} F_3 + \mu_1 F_1 \sum_{j=1}^{N} \beta_{\mathrm{SR},j}\right) \tag{144}$$

$$F_{11} = (1+\mu_1)(1+\mu_2) F_1, \tag{145}$$

and $\theta_{\diamond,i}$, $\varphi_{\diamond,i}$ and $\xi_{\diamond,i_1 i_2}$ are given in (16), (18) and (56), respectively.

Proof: See Appendix D.

For comparison, we next study the ideal scheme which the destinations can detect the signal based on the instantaneous CSI. With MRC/MRT and ZF processing, the achievable ergodic sum rates under AF strategy and full-duplex mode are given as

$$\tilde{\mathbf{S}}^{\diamond}_{\mathrm{FD,AF}} = \frac{T-\tau}{T} \sum_{n=1}^{N} \mathbb{E}\left\{\log_2\left(1+\widetilde{\mathrm{SINR}}_n^{\diamond}\right)\right\} \tag{146}$$

where

$$\widetilde{\mathrm{SINR}}_n^{\diamond} = \frac{\rho^2 P_{\mathrm{S}} P_{\mathrm{R}} \left|\mathbf{g}_{\mathrm{RD},n}^T \mathbf{F} \mathbf{g}_{\mathrm{SR},n}\right|^2}{\left(\begin{array}{l} \rho^2 P_{\mathrm{S}} P_{\mathrm{R}} \sum\limits_{j\neq n}^{N} \left|\mathbf{g}_{\mathrm{RD},n}^T \mathbf{F} \mathbf{g}_{\mathrm{SR},j}\right|^2 \\ +\rho^2 P_{\mathrm{R}} \left|\mathbf{g}_{\mathrm{RD},n}^T \mathbf{F} \mathbf{G}_{\mathrm{SR}} \mathbf{n}_1[i-1]\right|^2 \\ +\rho^2 P_{\mathrm{R}}^2 \left|\mathbf{g}_{\mathrm{RD},n}^T \mathbf{F} \mathbf{G}_{\mathrm{LI}} \tilde{\mathbf{y}}_{\mathrm{RT}}[i-1]\right|^2 \\ +\rho^2 P_{\mathrm{R}} \left|\mathbf{g}_{\mathrm{RD},n}^T \mathbf{F} \mathbf{G}_{\mathrm{LI}} \mathbf{n}_3[i-1]\right|^2 \\ +\rho^2 P_{\mathrm{R}} \left|\mathbf{g}_{\mathrm{RD},n}^T \mathbf{F} \mathbf{n}_{\mathrm{R}}[i-1]\right|^2 \\ +\rho^2 P_{\mathrm{R}} \left|\mathbf{g}_{\mathrm{RD},n}^T \mathbf{F} \mathbf{n}_2[i-1]\right|^2 \\ +\left|\mathbf{g}_{\mathrm{RD},n}^T \mathbf{n}_3[i]\right|^2 + \delta_{4,n} + 1 \end{array}\right)}. \tag{147}$$

B. AF POWER SCALING LAWS

Similar to the case of DF relaying, this subsection presents various power scaling laws for AF relaying in the limit of $N_{\mathrm{rx}} \to \infty$, $N_{\mathrm{tx}} \to \infty$ and $N_{\mathrm{rx}} = \kappa N_{\mathrm{tx}}$, $\kappa > 0$. As before, define $P_{\mathrm{S}} = \overline{P}_{\mathrm{S}}/N_{\mathrm{rx}}^a$, $P_{\mathrm{R}} = \overline{P}_{\mathrm{R}}/N_{\mathrm{tx}}^b$ and $P_{\mathrm{P}} = \overline{P}_{\mathrm{P}}/N_{\mathrm{rx}}^c$, where $a \geq 0$, $b \geq 0$ and $c \geq 0$.

First, with MRC/MRT and ZF processing, it is easy to see that the expressions in (118) and (133) tend to zero when $c > 1$, whereas they converge to a constant value when $c \leq 1$. The behaviors of (118) and (133) for other power scaling cases are presented in the following corollaries.

1) AF POWER SCALING LAWS OF MRC/MRT PROCESSING

Corollary 24: When $a + c < 1$ and $b + c < 1$, the sum spectral efficiency of MRC/MRT processing in (118) can be expressed as

$$\mathbf{S}^{\mathrm{MR}}_{\mathrm{FD,AF}} \to \frac{T-\tau}{T} \sum_{n=1}^{N} \log_2\left(1+\frac{\beta_{\mathrm{SR},n}^2 \beta_{\mathrm{RD},n}^2}{E_{12}}\right) \tag{148}$$

where

$$E_{12} = \sum_{j=1}^{N} \frac{(1+\lambda_1)(1+\mu_2)(N\lambda_{\mathrm{P}}+2\tau)\lambda_{\mathrm{P}} \beta_{\mathrm{RD},n}^2 \beta_{\mathrm{SR},j}^2}{\tau^2} + (\lambda_1+\mu_2+\lambda_1\mu_2)\beta_{\mathrm{SR},n}^2 \beta_{\mathrm{RD},n}^2. \tag{149}$$

Similar to Corollary 1, the above result also shows that, with the MRC/MRT processing and AF scheme, the sum spectral efficiency is not affected by the loop interference and relay's hardware impairments in this power scaling case.

Corollary 25: When $a = 1$, $b = 0$ and $c = 0$, the sum spectral efficiency of MRC/MRT processing in (118) can be expressed as

$$\mathbf{S}^{\mathrm{MR}}_{\mathrm{FD,AF}} \to \frac{T-\tau}{T} \sum_{n=1}^{N} \log_2\left(1+\frac{\overline{P}_{\mathrm{S}} \overline{P}_{\mathrm{R}} \beta_{\mathrm{SR},n}^2 \beta_{\mathrm{RD},n}^2}{\overline{P}_{\mathrm{R}}^2 E_{14} + \overline{P}_{\mathrm{S}} \overline{P}_{\mathrm{R}} E_{12} + \overline{P}_{\mathrm{R}} E_{13}}\right) \tag{150}$$

where

$$E_{13} = (1+\mu_1)(1+\mu_2)\left(\frac{\beta_{\mathrm{RD},n}^2 \sigma_{\mathrm{SR},n}^2 + \lambda_{\mathrm{P}} \beta_{\mathrm{RD},n}^2 \sum\limits_{j=1}^{N} \sigma_{\mathrm{SR},j}^2}{\tau}\right) \tag{151}$$

$$E_{14} = (1+\lambda_2)\sigma_{\mathrm{LI}}^2 E_{13}. \tag{152}$$

Corollary 26: When $a = 1$, $0 < b < 1$ and $c = 0$, the sum spectral efficiency of MRC/MRT processing in (118) can be expressed as

$$\mathbf{S}^{\mathrm{MR}}_{\mathrm{FD,AF}} \to \frac{T-\tau}{T} \sum_{n=1}^{N} \log_2\left(1+\frac{\overline{P}_{\mathrm{S}} \overline{P}_{\mathrm{R}} \beta_{\mathrm{SR},n}^2 \beta_{\mathrm{RD},n}^2}{\overline{P}_{\mathrm{S}} \overline{P}_{\mathrm{R}} E_{12} + \overline{P}_{\mathrm{R}} E_{13}}\right). \tag{153}$$

Similar to the MRC/MRT processing in the DF scheme, by comparing Corollary 25 and Corollary 26, one can see that power scaling in the relay's transmitter ($b > 0$) not only can save energy but also improve the rate performance in the AF scheme. This is also because the decrease of relay's power suppresses the impact of loop interference.

Corollary 27: When $a < 1$, $b = 1$ and $c = 0$, the sum spectral efficiency of MRC/MRT processing in (118) can be expressed as

$$\mathbf{S}^{\mathrm{MR}}_{\mathrm{FD,AF}} \to \frac{T-\tau}{T} \sum_{n=1}^{N} \log_2\left(1+\frac{\overline{P}_{\mathrm{S}} \overline{P}_{\mathrm{R}} \beta_{\mathrm{SR},n}^2 \beta_{\mathrm{RD},n}^2}{\overline{P}_{\mathrm{S}} \overline{P}_{\mathrm{R}} E_{12} + \overline{P}_{\mathrm{S}} E_{15}}\right) \tag{154}$$

where

$$E_{15} = (1+\lambda_1)(1+\mu_2) \sum_{j=1}^{N} \left(\frac{\sigma_{\mathrm{RD},j}^2 \beta_{\mathrm{SR},j}^2 + \lambda_{\mathrm{P}} \beta_{\mathrm{SR},j}^2 \sum\limits_{l=1}^{N} \sigma_{\mathrm{RD},l}^2}{\tau}\right). \tag{155}$$

Corollary 28: When $a = 1$, $b = 1$ and $c = 0$, the sum spectral efficiency of MRC/MRT processing in (118) can be

expressed as

$$\mathbf{S}_{\mathrm{FD,AF}}^{\mathrm{MR}} \to \frac{T-\tau}{T}\sum_{n=1}^{N}\log_2 \times\left(1+\frac{\overline{P}_{\mathrm{S}}\overline{P}_{\mathrm{R}}\beta_{\mathrm{SR},n}^2\beta_{\mathrm{RD},n}^2}{\overline{P}_{\mathrm{S}}\overline{P}_{\mathrm{R}}E_{12}+\overline{P}_{\mathrm{R}}E_{13}+\overline{P}_{\mathrm{S}}E_{15}+E_{11}}\right). \tag{156}$$

We can see that the rate in Corollary 27 is greater than that in Corollary 28. These two corollaries illustrate the effect of source's power scaling on the rate performance for MRC/MRT processing in the AF scheme.

Corollary 29: When $a+c=1$, $b=0$ and $0<c<1$, the sum spectral efficiency of MRC/MRT processing in (118) can be expressed as

$$\mathbf{S}_{\mathrm{FD,AF}}^{\mathrm{MR}} \to \frac{T-\tau}{T}\sum_{n=1}^{N}\log_2\left(1+\frac{\overline{P}_{\mathrm{S}}\overline{P}_{\mathrm{R}}\beta_{\mathrm{SR},n}^2\beta_{\mathrm{RD},n}^2}{\overline{P}_{\mathrm{R}}^2E_{17}+\overline{P}_{\mathrm{S}}\overline{P}_{\mathrm{R}}E_{12}+\overline{P}_{\mathrm{R}}E_{16}}\right) \tag{157}$$

where

$$E_{16}=\frac{(1+\mu_1)(1+\mu_2)(1+\mu_{\mathrm{P}})(N\lambda_{\mathrm{P}}+\tau)\beta_{\mathrm{RD},n}^2}{\tau^2\overline{P}_{\mathrm{P}}} \tag{158}$$

$$E_{17}=(1+\lambda_2)\sigma_{\mathrm{LI}}^2E_{16}. \tag{159}$$

Corollary 30: When $a+c=1$ and $0<b<a<1$, the sum spectral efficiency of MRC/MRT processing in (118) can be expressed as

$$\mathbf{S}_{\mathrm{FD,AF}}^{\mathrm{MR}} \to \frac{T-\tau}{T}\sum_{n=1}^{N}\log_2\left(1+\frac{\overline{P}_{\mathrm{S}}\overline{P}_{\mathrm{R}}\beta_{\mathrm{SR},n}^2\beta_{\mathrm{RD},n}^2}{\overline{P}_{\mathrm{S}}\overline{P}_{\mathrm{R}}E_{12}+\overline{P}_{\mathrm{R}}E_{16}}\right). \tag{160}$$

By comparing Corollary 29 and Corollary 30, it is also seen that power scaling in the relay's transmitter ($b>0$) helps to save energy and improve the system performance for the MRC/MRT processing in the AF scheme.

Corollary 31: When $a+c<1$, $b+c=1$ and $c>0$, the sum spectral efficiency of MRC/MRT processing in (118) can be expressed as

$$\mathbf{S}_{\mathrm{FD,AF}}^{\mathrm{MR}} \to \frac{T-\tau}{T}\sum_{n=1}^{N}\log_2\left(1+\frac{\overline{P}_{\mathrm{S}}\overline{P}_{\mathrm{R}}\beta_{\mathrm{SR},n}^2\beta_{\mathrm{RD},n}^2}{\overline{P}_{\mathrm{S}}\overline{P}_{\mathrm{R}}E_{12}+\overline{P}_{\mathrm{S}}E_{18}}\right) \tag{161}$$

where

$$E_{18}=\frac{(1+\lambda_1)(1+\mu_2)(1+\mu_{\mathrm{P}})(N\lambda_{\mathrm{P}}+\tau)\kappa^c\sum_{j=1}^{N}\beta_{\mathrm{SR},j}^2}{\tau^2\overline{P}_{\mathrm{P}}}. \tag{162}$$

Corollary 32: When $a+c=1$, $b+c=1$ and $0<c<1$, the sum spectral efficiency of MRC/MRT processing in (118) can be expressed as

$$\mathbf{S}_{\mathrm{FD,AF}}^{\mathrm{MR}} \to \frac{T-\tau}{T}\sum_{n=1}^{N} \times\log_2\left(1+\frac{\overline{P}_{\mathrm{S}}\overline{P}_{\mathrm{R}}\beta_{\mathrm{SR},n}^2\beta_{\mathrm{RD},n}^2}{\overline{P}_{\mathrm{S}}\overline{P}_{\mathrm{R}}E_{12}+\overline{P}_{\mathrm{R}}E_{16}+\overline{P}_{\mathrm{S}}E_{18}+E_{19}}\right) \tag{163}$$

where

$$E_{19}=\frac{(1+\mu_1)(1+\mu_2)(1+\mu_{\mathrm{P}})^2N\kappa^c}{\tau^2\overline{P}_{\mathrm{P}}^2}. \tag{164}$$

Comparing (161) and (163) revels that the rate in (161) is greater than the rate in (163).

Corollary 33: When $a=0$, $b=0$ and $c=1$, the sum spectral efficiency of MRC/MRT processing in (118) can be expressed as

$$\mathbf{S}_{\mathrm{FD,AF}}^{\mathrm{MR}} \to \frac{T-\tau}{T}\sum_{n=1}^{N}\log_2 \times\left(1+\frac{\overline{P}_{\mathrm{S}}\overline{P}_{\mathrm{R}}\beta_{\mathrm{SR},n}^2\beta_{\mathrm{RD},n}^2}{\overline{P}_{\mathrm{R}}^2E_{20}+\overline{P}_{\mathrm{S}}\overline{P}_{\mathrm{R}}E_{21}+\overline{P}_{\mathrm{R}}E_{22}+\overline{P}_{\mathrm{S}}E_{23}+E_{19}}\right) \tag{165}$$

where

$$E_{20}=(1+\lambda_2)^2\beta_{\mathrm{RD},n}\sigma_{\mathrm{LI}}^2E_{19}+E_{17} \tag{166}$$

$$E_{21}=(1+\lambda_1)\left((1+\lambda_2)\beta_{\mathrm{RD},n}E_{19}+E_{16}\right)\sum_{j=1}^{N}\beta_{\mathrm{SR},j} +(1+\lambda_2)\beta_{\mathrm{RD},n}E_{18} +\frac{(1+\lambda_1)(1+\mu_2)(N\lambda_{\mathrm{P}}+2\tau)\lambda_{\mathrm{P}}\beta_{\mathrm{RD},n}^2\sum_{j=1}^{N}\beta_{\mathrm{SR},j}^2}{\tau^2} +(\lambda_1+\mu_2+\lambda_1\mu_2)\beta_{\mathrm{SR},n}^2\beta_{\mathrm{RD},n}^2 \tag{167}$$

$$E_{22}=(1+\lambda_2)\left(\beta_{\mathrm{RD},n}+\sigma_{\mathrm{LI}}^2\right)E_{19}+E_{16} \tag{168}$$

$$E_{23}=(1+\lambda_1)E_{19}\sum_{j=1}^{N}\beta_{\mathrm{SR},j}+E_{18}. \tag{169}$$

The results presented in Corollary 24 to Corollary 33 provide various power scaling laws in terms of different coefficients ($a, b, c \geq 0$, $a+c \leq 1$ and $b+c \leq 1$) for the MRC/MRT processing under the AF scheme. It can be concluded that the impact of loop interference can be eliminated in the case with $b>0$. In general, these corollaries show that scaling of the transmit power of the relay station can reduce the effect of loop interference and save energy, while maintaining the system performance.

2) AF POWER SCALING LAWS OF ZF PROCESSING

Corollary 34: When $0 \leq a, b < 1$ and $c = 0$, the sum spectral efficiency of ZF processing in (133) can be expressed as

$$\mathbf{S}_{\mathrm{FD,AF}}^{\mathrm{ZF}} \to \frac{T-\tau}{T} \sum_{n=1}^{N} \log_2 \left(1 + \frac{\theta_{\mathrm{SR},n}^2}{F_{13}}\right) \tag{170}$$

where

$$F_{12} = \sum_{j=1}^{N}\sum_{i=1}^{N} \frac{\lambda_{\mathrm{P}}^2 \theta_{\mathrm{SR},j}^2 \theta_{\mathrm{SR},i}^2 \theta_{\mathrm{RD},i}^2}{\tau^2} + \sum_{j=1}^{N} \frac{\lambda_{\mathrm{P}} \theta_{\mathrm{SR},j}^2 \theta_{\mathrm{SR},n}^2}{\tau} + \sum_{j=1}^{N} \frac{\lambda_{\mathrm{P}} \theta_{\mathrm{SR},j}^2 \theta_{\mathrm{RD},j}^2}{\tau} \tag{171}$$

$$F_{13} = (1+\lambda_1)(1+\mu_2) F_{12} + (\lambda_1 + \mu_2 + \lambda_1 \mu_2) \theta_{\mathrm{SR},n}^2. \tag{172}$$

Corollary 35: When $a + c < 1$, $b + c < 1$, $0 \leq a, b < 1$ and $0 < c < 1$, the sum spectral efficiency of ZF processing in (133) can be expressed as

$$\mathbf{S}_{\mathrm{FD,AF}}^{\mathrm{ZF}} \to \frac{T-\tau}{T} \sum_{n=1}^{N} \log_2 \left(1 + \frac{1}{\lambda_1 + \mu_2 + \lambda_1 \mu_2}\right). \tag{173}$$

With ZF processing in the AF strategy, Corollary 34 and Corollary 35 reveal the effect of pilot power on the system performance. Different from Corollary 24, when $a + c < 1$, $b + c < 1$ and $0 < c < 1$, the effect of hardware impairment of λ_{P} and μ_{P} can disappear and $\mathbf{S}_{\mathrm{FD,AF}}^{\mathrm{ZF}} \geq \mathbf{S}_{\mathrm{FD,AF}}^{\mathrm{MR}}$ in the power scaling case of $a + c < 1$, $b + c < 1$ and $0 \leq a, b < 1$. This shows that, under the AF strategy, ZF processing performs better than MRC/MRT processing in this power scaling case.

Corollary 36: When $a = 1$, $b = 0$ and $c = 0$, the sum spectral efficiency of ZF processing in (133) can be expressed as

$$\mathbf{S}_{\mathrm{FD,AF}}^{\mathrm{ZF}} \to \frac{T-\tau}{T} \sum_{n=1}^{N} \log_2 \left(1 + \frac{\bar{P}_{\mathrm{S}} \bar{P}_{\mathrm{R}} \theta_{\mathrm{SR},n}^2}{\bar{P}_{\mathrm{R}}^2 F_{15} + \bar{P}_{\mathrm{S}} \bar{P}_{\mathrm{R}} F_{13} + \bar{P}_{\mathrm{R}} F_{14}}\right) \tag{174}$$

where

$$F_{14} = \sum_{j=1}^{N} (1+\mu_1) \left(\frac{\lambda_{\mathrm{P}} \theta_{\mathrm{RD},j}^2}{\tau} + \delta(n,j)\right) \times (1+\mu_2) \left(\frac{1}{\eta_{\mathrm{SR},j}} + \frac{\lambda_{\mathrm{P}} \theta_{\mathrm{SR},j}^2 \sum_{i=1}^{N} \eta_{\mathrm{SR},i}^{-1}}{\tau}\right) \tag{175}$$

$$F_{15} = (1+\lambda_2) \sigma_{\mathrm{LI}}^2 F_{14}. \tag{176}$$

Corollary 37: When $a = 1$, $0 < b < 1$ and $c = 0$, the sum spectral efficiency of ZF processing in (133) can be expressed as

$$\mathbf{S}_{\mathrm{FD,AF}}^{\mathrm{ZF}} \to \frac{T-\tau}{T} \sum_{n=1}^{N} \log_2 \left(1 + \frac{\bar{P}_{\mathrm{S}} \bar{P}_{\mathrm{R}} \theta_{\mathrm{SR},n}^2}{\bar{P}_{\mathrm{S}} \bar{P}_{\mathrm{R}} F_{13} + \bar{P}_{\mathrm{R}} F_{14}}\right). \tag{177}$$

From Corollary 36 and Corollary 37, we can see a similar phenomenon as in the case of DF relaying, namely power scaling in the relay's transmitter ($b > 0$) helps to save energy and improve the rate performance for the ZF processing under the AF scheme. This is also because reducing the relay's transmit power helps to suppress the loop interference.

Corollary 38: When $a < 1$, $b = 1$ and $c = 0$, the sum spectral efficiency of ZF processing in (133) can be expressed as

$$\mathbf{S}_{\mathrm{FD,AF}}^{\mathrm{ZF}} \to \frac{T-\tau}{T} \sum_{n=1}^{N} \log_2 \left(1 + \frac{\bar{P}_{\mathrm{S}} \bar{P}_{\mathrm{R}} \theta_{\mathrm{SR},n}^2 \theta_{\mathrm{RD},n}^2}{\bar{P}_{\mathrm{S}} \bar{P}_{\mathrm{R}} F_{13} \theta_{\mathrm{RD},n}^2 + \bar{P}_{\mathrm{S}} F_{16}}\right) \tag{178}$$

where

$$F_{16} = \sum_{j=1}^{N}\sum_{i=1}^{N} (1+\lambda_1) \left(\frac{\lambda_{\mathrm{P}} \theta_{\mathrm{SR},j}^2 \theta_{\mathrm{SR},i}^2}{\tau} + \theta_{\mathrm{SR},j}^2 \delta(j,i)\right) \times (1+\mu_2) \left(\frac{1}{\eta_{\mathrm{RD},i}} + \frac{\lambda_{\mathrm{P}} \theta_{\mathrm{RD},i}^2 \sum_{l=1}^{N} \eta_{\mathrm{RD},l}^{-1}}{\tau}\right). \tag{179}$$

Corollary 39: When $a = 1$, $b = 1$ and $c = 0$, the sum spectral efficiency of ZF processing in (133) can be expressed as

$$\mathbf{S}_{\mathrm{FD,AF}}^{\mathrm{ZF}} \to \frac{T-\tau}{T} \sum_{n=1}^{N} \log_2 \times \left(1 + \frac{\bar{P}_{\mathrm{S}} \bar{P}_{\mathrm{R}} \theta_{\mathrm{SR},n}^2 \theta_{\mathrm{RD},n}^2}{\bar{P}_{\mathrm{S}} \bar{P}_{\mathrm{R}} F_{13} \theta_{\mathrm{RD},n}^2 + \bar{P}_{\mathrm{R}} F_{14} \theta_{\mathrm{RD},n}^2 + \bar{P}_{\mathrm{S}} F_{16} + F_{17}}\right). \tag{180}$$

where

$$F_{17} = \sum_{j=1}^{N} (1+\mu_1) \left(\frac{1}{\eta_{\mathrm{RD},j}} + \frac{\lambda_{\mathrm{P}} \theta_{\mathrm{RD},j}^2 \sum_{i=1}^{N} \eta_{\mathrm{RD},i}^{-1}}{\tau}\right) \times (1+\mu_2) \left(\frac{1}{\eta_{\mathrm{SR},j}} + \frac{\lambda_{\mathrm{P}} \theta_{\mathrm{SR},j}^2 \sum_{i=1}^{N} \eta_{\mathrm{SR},i}^{-1}}{\tau}\right). \tag{181}$$

We can see that the rate in (178) is greater than the rate in (180). Thus Corollary 38 and Corollary 39 illustrate the effect of source power scaling on the rate performance for ZF processing in the AF scheme.

Corollary 40: When $a + c = 1$, $b = 0$ and $0 < c < 1$, the sum spectral efficiency of ZF processing in (133) can be expressed as

$$\mathbf{S}_{\mathrm{FD,AF}}^{\mathrm{ZF}} \to \frac{T-\tau}{T} \sum_{n=1}^{N} \log_2 \left(1 + \frac{\bar{P}_{\mathrm{S}} \bar{P}_{\mathrm{R}} F_{19}}{\bar{P}_{\mathrm{R}}^2 F_{20} + \bar{P}_{\mathrm{S}} \bar{P}_{\mathrm{R}} F_{21} + \bar{P}_{\mathrm{R}} F_{22}}\right) \tag{182}$$

where

$$F_{18} = \frac{\tau \bar{P}_{\mathrm{P}}}{1+\mu_{\mathrm{P}}} \tag{183}$$

$$F_{19} = \beta_{\mathrm{SR},n}^2 F_{18} \tag{184}$$

$$F_{20} = (1+\lambda_2)(1+\mu_1)(1+\mu_2)\sigma_{\mathrm{LI}}^2 \tag{185}$$

$$F_{21} = (\lambda_1+\mu_2+\lambda_1\mu_2) F_{19} \tag{186}$$

$$F_{22} = (1+\mu_1)(1+\mu_2). \tag{187}$$

Corollary 41: When $a+c=1$ and $0<b<a<1$, the sum spectral efficiency of ZF processing in (133) can be expressed as

$$\mathbf{S}_{\mathrm{FD,AF}}^{\mathrm{ZF}} \to \frac{T-\tau}{T}\sum_{n=1}^{N}\log_2\left(1+\frac{\bar{P}_{\mathrm{S}}\bar{P}_{\mathrm{R}}F_{19}}{\bar{P}_{\mathrm{S}}\bar{P}_{\mathrm{R}}F_{21}+\bar{P}_{\mathrm{R}}F_{22}}\right). \tag{188}$$

Corollary 40 and Corollary 41 once again verify that power scaling in the relay's transmitter ($b>0$) helps to save energy and improve the system performance for the ZF processing in the AF scheme.

Corollary 42: When $a+c<1$, $b+c=1$ and $c>0$, the sum spectral efficiency of ZF processing in (133) can be expressed as

$$\mathbf{S}_{\mathrm{FD,AF}}^{\mathrm{ZF}} \to \frac{T-\tau}{T}\sum_{n=1}^{N}\log_2\left(1+\frac{\bar{P}_{\mathrm{S}}\bar{P}_{\mathrm{R}}F_{19}\beta_{\mathrm{RD},n}^2}{\bar{P}_{\mathrm{S}}\bar{P}_{\mathrm{R}}F_{21}\beta_{\mathrm{RD},n}^2+\bar{P}_{\mathrm{S}}F_{23}}\right) \tag{189}$$

where

$$F_{23} = (1+\lambda_1)(1+\mu_2)\kappa^c\sum_{j=1}^{N}\beta_{\mathrm{SR},j}^2. \tag{190}$$

Corollary 43: When $a+c=1$, $b+c=1$ and $0<c<1$, the sum spectral efficiency of ZF processing in (133) can be expressed as

$$\mathbf{S}_{\mathrm{FD,AF}}^{\mathrm{ZF}} \to \frac{T-\tau}{T}\sum_{n=1}^{N}\log_2 \times\left(1+\frac{\bar{P}_{\mathrm{S}}\bar{P}_{\mathrm{R}}F_{19}\beta_{\mathrm{RD},n}^2}{\bar{P}_{\mathrm{S}}\bar{P}_{\mathrm{R}}F_{21}\beta_{\mathrm{RD},n}^2+\bar{P}_{\mathrm{R}}F_{22}\beta_{\mathrm{RD},n}^2+\bar{P}_{\mathrm{S}}F_{23}+F_{24}}\right) \tag{191}$$

where

$$F_{24} = \frac{(1+\mu_1)(1+\mu_2)(1+\mu_{\mathrm{P}})N\kappa^c}{\tau\bar{P}_{\mathrm{P}}}. \tag{192}$$

Comparing Corollary 42 and Corollary 43 shows that the rate in Corollary 42 is greater than the rate in Corollary 43.

Corollary 44: When $a=0$, $b=0$ and $c=1$, the sum spectral efficiency of ZF processing in (133) can be expressed as

$$\mathbf{S}_{\mathrm{FD,AF}}^{\mathrm{ZF}} \to \frac{T-\tau}{T}\sum_{n=1}^{N}\log_2 \times\left(1+\frac{\bar{P}_{\mathrm{S}}\bar{P}_{\mathrm{R}}F_{27}}{\bar{P}_{\mathrm{R}}^2F_{29}+\bar{P}_{\mathrm{S}}\bar{P}_{\mathrm{R}}F_{30}+\bar{P}_{\mathrm{R}}F_{31}+\bar{P}_{\mathrm{S}}F_{32}+F_{33}}\right) \tag{193}$$

$$F_{25} = \beta_{\mathrm{RD},n}^2 F_{18} + N\beta_{\mathrm{RD},n}\kappa^c \tag{194}$$

$$F_{26} = \sum_{j=1}^{N}\kappa^c\left(\beta_{\mathrm{SR},j}^2 F_{18}+N\beta_{\mathrm{SR},j}\right) \tag{195}$$

$$F_{27} = \beta_{\mathrm{SR},n}^2\beta_{\mathrm{RD},n}^2 F_{18}^2 \tag{196}$$

$$F_{28} = \sum_{j=1}^{N}\sum_{i=1}^{N}\left(\kappa^c\beta_{\mathrm{RD},n}+\beta_{\mathrm{RD},n}^2F_{18}\delta(n,i)\right) \times\left(\beta_{\mathrm{SR},j}+\beta_{\mathrm{SR},j}^2F_{18}\delta(j,i)\right) \tag{197}$$

$$F_{29} = (1+\lambda_2)\left(N\lambda_2\beta_{\mathrm{RD},n}\kappa^c+F_{25}\right)\sigma_{\mathrm{LI}}^2F_{22} \tag{198}$$

$$F_{30} = (1+\lambda_1)(1+\mu_2)\left(F_{28}+\lambda_2\beta_{\mathrm{RD},n}F_{26} + \left(N\lambda_2\mu_1\beta_{\mathrm{RD},n}\kappa^c+\mu_1F_{25}\right)\sum_{j=1}^{N}\beta_{\mathrm{SR},j}\right)-F_{27} \tag{199}$$

$$F_{31} = \left(F_{25}+N\kappa^c\left((1+\lambda_2)\sigma_{\mathrm{LI}}^2+\lambda_2\beta_{\mathrm{RD},n}\right)\right)F_{22} \tag{200}$$

$$F_{32} = (1+\lambda_1)(1+\mu_2)\left(F_{26}+N\mu_1\kappa^c\sum_{j=1}^{N}\beta_{\mathrm{SR},j}\right) \tag{201}$$

$$F_{33} = N\kappa^cF_{22}. \tag{202}$$

In summary, Corollary 34 to Corollary 44 provide many power scaling laws for ZF processing in the AF scheme ($a,b,c\geq 0$, $a+c\leq 1$ and $b+c\leq 1$). An important result is that scaling the power of the relay's transmitter ($b>0$) can eliminate the influence of the loop interference and improve the system performance for ZF processing in the AF scheme. In the power scaling case with $a+c<1$, $b+c<1$, $0\leq a,b<1$ and $0<c<1$, the hardware impairments of λ_{P} and μ_{P} do not affect the rate performance.

C. AF HALF-DUPLEX SCENARIO

Following the same reasoning as in Corollary 22 and Corollary 23 in the DF scheme, we can obtain Corollary 45 and Corollary 46 which give the sum spectral efficiencies of the half-duplex AF relaying systems with MRC/MRT and ZF processing.

Corollary 45: The sum spectral efficiency of the half-duplex AF relaying with MRC/MRT processing is given by

$$\mathbf{S}_{\mathrm{HD,AF}}^{\mathrm{MR}}=\frac{T-\tau}{2T}\sum_{n=1}^{N}\log_2\left(1+\frac{4P_{\mathrm{R}}P_{\mathrm{S}}E_4}{\left(\begin{array}{c}4P_{\mathrm{R}}P_{\mathrm{S}}E_8+2P_{\mathrm{R}}E_{24}\\+2P_{\mathrm{S}}E_{10}+E_{11}\end{array}\right)}\right) \tag{203}$$

where

$$E_{24}=(1+\mu_1)(1+\mu_2)\left(E_2+\lambda_2\beta_{\mathrm{RD},n}E_1\right). \tag{204}$$

Corollary 46: The sum spectral efficiency of the half-duplex AF relaying with ZF processing can be given by

$$\mathbf{S}_{\mathrm{HD,AF}}^{\mathrm{ZF}}=\frac{T-\tau}{2T}\sum_{n=1}^{N}\log_2\left(1+\frac{4P_{\mathrm{R}}P_{\mathrm{S}}F_4}{\left(\begin{array}{c}4P_{\mathrm{R}}P_{\mathrm{S}}F_8+2P_{\mathrm{R}}F_{34}\\+2P_{\mathrm{S}}F_{10}+F_{11}\end{array}\right)}\right) \tag{205}$$

where

$$F_{34}=(1+\mu_1)(1+\mu_2)\left(F_2+\lambda_2\beta_{\mathrm{RD},n}F_1\right). \tag{206}$$

Based on Corollary 45 and Corollary 46, various power scaling properties of the half-duplex AF relaying with MRC/MRT and ZF processing can be easily obtained, but they are omitted here.

From Corollary 1 to Corollary 46, it is observed that the power scaling in relay ($b > 0$) is the only way to improve system performance while reducing transmit energy in the different power scaling for sources, relay and pilot. Therefore we can conclude that the power scaling in relay is very suitable for practical applications in the FDR system with hardware impairment. Before closing this section, it is pointed out that the power scaling laws for MRC/MRT and ZF processing in the DF and AF schemes studied in Sections III and IV are all under the case of equal relay's transmit powers. However, it is known that proper power allocation and the optimization of relay beamforming can improve the spectral efficiency and energy efficiency of communication networks. In particular, in massive MIMO, power allocation can break the limitations from the assumption of equal transmit power among relay's transmitter, and contribute much to harvest all the benefits brought by the large antenna arrays. Research on power allocation and the optimization of relay beamforming have attracted strong interests in recent years [17], [25], [33], but this issue is beyond the scope of this paper and left for further studies.

V. NUMERICAL RESULTS AND DISCUSSION

This section presents numerical results to corroborate the analytical results obtained in the previous two sections. In all illustrative examples, it is assumed that $T = 200$, $N = 5$, $\tau = N$, $\mathbf{D}_{\mathrm{SR}} = \mathbf{D}_{\mathrm{RD}} = \mathbf{I}_N$ and $N_{\mathrm{rx}} = N_{\mathrm{tx}}$. Furthermore, the factors that quantify the quality of transceiver hardware are set as $\lambda_1 = \lambda_{\mathrm{P}} = \mu_2 = v$ for sources and destinations, and

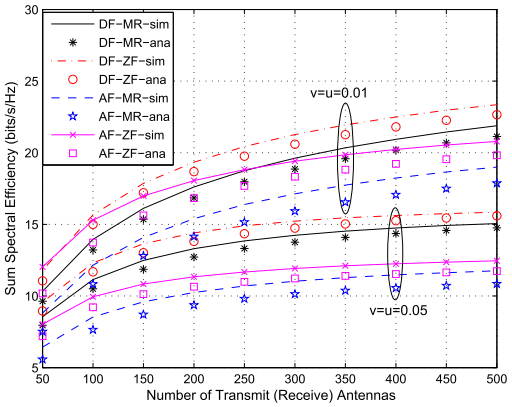

FIGURE 2. Effect of the number of relay's antennas on the sum spectral efficiency for massive MIMO full-duplex relaying: $P_{\mathrm{R}} = P_{\mathrm{P}} = P_{\mathrm{S}} = 10$dB, $\sigma_{\mathrm{LI}}^2 = 10$dB.

$\lambda_2 = \mu_{\mathrm{P}} = \mu_1 = u$ for the relay. Their values can be chosen to be higher than 0.175^2 in order to examine the possibility of using low-quality hardware [32].

A. ACHIEVABLE RATE PERFORMANCE

For both DF and AF schemes, Fig. 2 compares the closed-form lower bounds of the sum spectral efficiencies of MRC/MRT or ZF processing based on (43), (53), (118) and (133) with numerical results based on (62) and (146). Here, the sum spectral efficiencies are plotted versus the number of antennas for different levels of hardware impairments. In this example, it is assumed that $P_{\mathrm{R}} = P_{\mathrm{P}} = P_{\mathrm{S}} = 10$dB and $\sigma_{\mathrm{LI}}^2 = 10$dB. Clearly, all the lower bounds appear tight to the numerical results, which suggests the tightness of the lower bounds to the exact sum spectral efficiencies. For both DF and AF schemes, when the level of hardware impairments increases, the sum spectral efficiencies of MRC/MRT and ZF processing significantly decrease. When the number of antennas grows large, it can also be seen that (i) the rate performance gradually increases, (ii) the DF scheme outperforms the AF scheme, and (iii) the performance of ZF processing is better than that of MRC/MRT processing. Given the tightness between the lower bounds and the numerically-evaluated sum spectral efficiencies, only the theoretical lower bound expressions are used in the following examples.

With MRC/MRT or ZF processing, Fig. 3 compares the sum spectral efficiencies of massive MIMO DF and AF FDR systems for different loop interference levels and hardware impairments. Here it is assumed that $P_{\mathrm{R}} = P_{\mathrm{P}} = P_{\mathrm{S}} = 10$dB and $N_{\mathrm{rx}} = N_{\mathrm{tx}} = 100$. A key observation from the figure is that, at a low level of loop interference, the hardware quality at the sources and destinations has a stronger impact on the system's rate performance than the hardware quality at the relay. Specifically, compared with using high-quality hardware at the relay, the sum spectral efficiencies can be greatly improved by using high-quality hardware at sources and destinations. At a high level of loop interference, the hardware quality of sources, destinations and the relay have basically

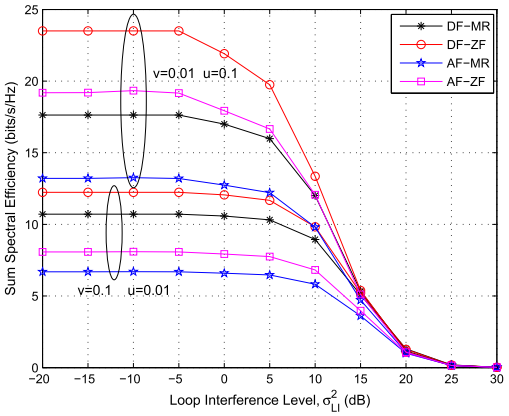

FIGURE 3. Effect of loop interference level on the sum spectral efficiency for massive MIMO full-duplex relaying: $P_R = P_P = P_S = 10$dB and $N_{rx} = N_{tx} = 100$.

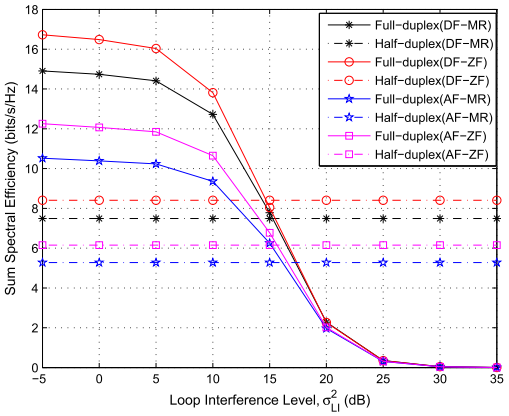

FIGURE 4. Effect of loop interference level on the sum spectral efficiency for massive MIMO full-duplex and half-duplex relaying: $P_R = P_P = P_S = 10$dB, $N_{rx} = N_{tx} = 200$, $v = 0.05$ and $u = 0.05$.

the same impact on the spectral efficiencies. In addition, when the level of loop interference is small, it can also be seen that, compared to MRC/MRT processing, ZF processing achieves larger performance improvement in the case of high-quality hardware at the sources and destinations under both DF and AF schemes.

B. FULL-DUPLEX RELAYING VERSUS HALF-DUPLEX RELAYING

With MRC/MRT or ZF processing, Fig. 4 compares the sum spectral efficiencies of FDR based on (43), (53), (118) and (133) with the sum spectral efficiencies of half-duplex relaying (HDR) based on (105), (106), (203) and (205) for different levels of loop interference under DF and AF schemes. In this figure, the parameters are set as follows $P_R = P_P = P_S = 10$dB, $N_{rx} = N_{tx} = 200$, $v = 0.05$ and $u = 0.05$. As expected, the sum spectral efficiencies of MRC/MRT and ZF processing in the full-duplex mode for both DF and AF schemes decrease as the level of loop interference grows and the sum spectral efficiency of the DF scheme is greater than that of the AF scheme. It can be seen that the full-duplex

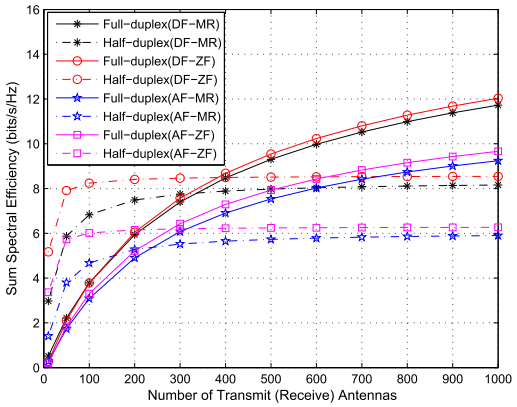

FIGURE 5. Effect of the number of relay's antennas on the sum spectral efficiency for massive MIMO full-duplex and half-duplex relaying: $P_R = P_P = P_S = 10$dB, $\sigma^2_{LI} = 20$dB, $v = 0.05$ and $u = 0.05$.

mode outperforms the half-duplex mode when σ^2_{LI} is small, while the opposite is true when σ^2_{LI} is large. It can also be seen that using large-scale antenna arrays at the relay can suppress the effect of loop interference. This implies that, when the number of relay's antennas is large, the full-duplex mode is more attractive than the half-duplex mode. The effect of the number of relaying antennas on the sum spectral efficiency can be clearly observed in Fig. 5. From Fig. 4 and 5, one can also find that, under both DF and AF schemes, MRC/MRT processing can take advantage of the full-duplex mode better than ZF processing when there are larger loop interference level and smaller number of relay's antennas.

C. POWER SCALING

Among the scenarios examined in various corollaries, the following four typical cases are chosen to observe power scaling behaviors:

Case 1: $P_S = \frac{\overline{P}_S}{N_{rx}^1}$, $P_R = \frac{\overline{P}_R}{N_{tx}^0}$ and $P_P = \frac{\overline{P}_P}{N_{rx}^0}$;

Case 2: $P_S = \frac{\overline{P}_S}{N_{rx}^1}$, $P_R = \frac{\overline{P}_R}{N_{tx}^{\frac{1}{2}}}$ and $P_P = \frac{\overline{P}_P}{N_{rx}^0}$;

Case 3: $P_S = \frac{\overline{P}_S}{N_{rx}^{\frac{1}{2}}}$, $P_R = \frac{\overline{P}_R}{N_{tx}^0}$ and $P_P = \frac{\overline{P}_P}{N_{rx}^{\frac{1}{2}}}$;

Case 4: $P_S = \frac{\overline{P}_S}{N_{rx}^{\frac{1}{2}}}$, $P_R = \frac{\overline{P}_R}{N_{tx}^{\frac{1}{3}}}$ and $P_P = \frac{\overline{P}_P}{N_{rx}^{\frac{1}{2}}}$;

Let $\overline{P}_P = \overline{P}_S = \overline{P}_R = 10$dB, $\sigma^2_{LI} = 1$dB, $v = 0.05$ and $u = 0.05$. The sum spectral efficiency curves of DF scheme for four cases are plotted in Fig. 6 and Fig. 7 for MRC/MRT and ZF processing, respectively. The sum spectral efficiency curves of the AF scheme for four cases are plotted in Fig. 8 and Fig. 9 for MRC/MRT and ZF processing, respectively. It is clear from Figs. 6 to 9 that as N_{rx} and N_{tx} grow large, all of the four sum spectral efficiency curves approach to their corresponding constant asymptotical rates. It should be pointed out that our asymptotical results under Cases 1 to 4 are certainly accurate when the number of relay's antennas is very large. The results in those figures indicate that the asymptotic analysis given in the paper is also accurate and valid for finite numbers of antennas. Under both DF and

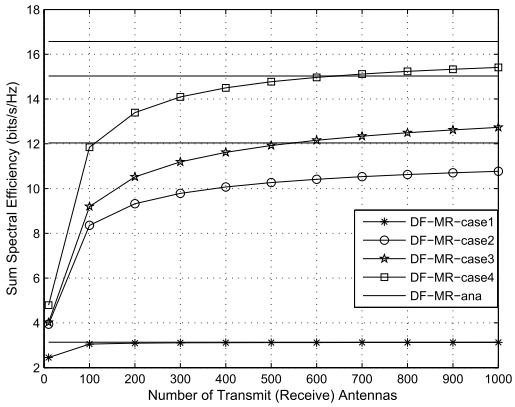

FIGURE 6. Effect of the number of relay's antennas on the sum spectral efficiency for massive MIMO DF full-duplex relaying with MRC/MRT processing under different scaling laws: $\bar{P}_{\mathrm{R}} = \bar{P}_{\mathrm{P}} = \bar{P}_{\mathrm{S}} = 10\mathrm{dB}$, $\sigma^2_{\mathrm{LI}} = 1\mathrm{dB}$, $v = 0.05$ and $u = 0.05$.

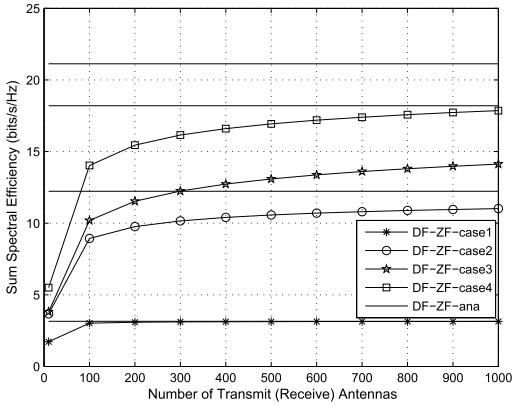

FIGURE 7. Effect of the number of relay's antennas on the sum spectral efficiency for massive MIMO DF full-duplex relaying with ZF processing under different scaling laws: $\bar{P}_{\mathrm{R}} = \bar{P}_{\mathrm{P}} = \bar{P}_{\mathrm{S}} = 10\mathrm{dB}$, $\sigma^2_{\mathrm{LI}} = 1\mathrm{dB}$, $v = 0.05$ and $u = 0.05$.

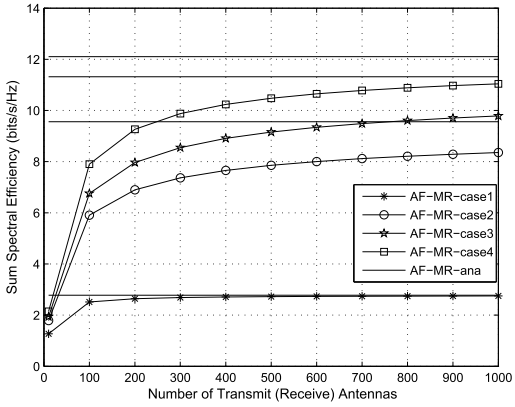

FIGURE 8. Effect of the number of relay's antennas on the sum spectral efficiency for massive MIMO AF full-duplex relaying with MRC/MRT processing under different scaling laws: $\bar{P}_{\mathrm{R}} = \bar{P}_{\mathrm{P}} = \bar{P}_{\mathrm{S}} = 10\mathrm{dB}$, $\sigma^2_{\mathrm{LI}} = 1\mathrm{dB}$, $v = 0.05$ and $u = 0.05$.

AF schemes, it can also be observed that the sum spectral efficiency in Case 2 is greater than that in Case 1 and the sum spectral efficiency in Case 4 is greater than that in Cases 3 for both of MRC/MRT and ZF processing. Such relative performance comparison agrees with related corollaries given before. Based on numerical results and theoretical analysis, it can be seen that Case 2 and Case 4 offer an attractive power scaling property in terms of energy efficiency and spectral efficiency. Finally, by comparing Fig. 6 and Fig. 7 with Fig. 8 and Fig. 9, it is seen that the DF scheme can provide better rate performance than the AF scheme for MRC/MRT and ZF processing under the various cases of power scaling.

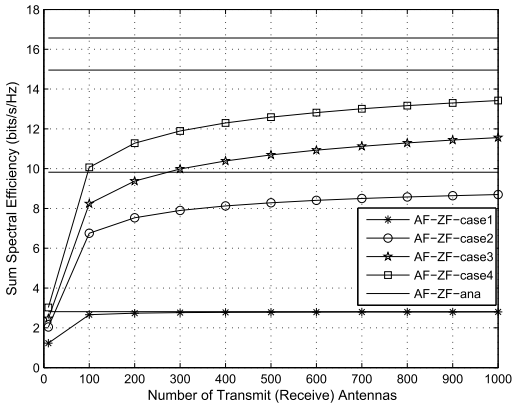

FIGURE 9. Effect of the number of relay's antennas on the sum spectral efficiency for massive MIMO AF full-duplex relaying with ZF processing under different scaling laws: $\bar{P}_{\mathrm{R}} = \bar{P}_{\mathrm{P}} = \bar{P}_{\mathrm{S}} = 10\mathrm{dB}$, $\sigma^2_{\mathrm{LI}} = 1\mathrm{dB}$, $v = 0.05$ and $u = 0.05$.

VI. CONCLUSIONS

This paper studied the sum spectral efficiencies of massive MIMO DF and AF FDR systems with MRC/MRT or ZF operating over Rayleigh fading channels. Under the scenario of imperfect CSI, closed-form expressions of their lower bounds were derived and various power scaling laws were presented. Numerical results illustrated that the derived rate expressions are very accurate. It has been showed that, when $N_{\mathrm{rx}}, N_{\mathrm{tx}} \to \infty$ with a fixed ratio, the transmit powers of sources, relay and pilots can be scaled down by $1/N^a_{\mathrm{rx}}$, $1/N^b_{\mathrm{tx}}$ and $1/N^c_{\mathrm{rx}}$, respectively (where $a, b, c \geq 0$, $a + c \leq 1$ and $b + c \leq 1$) without compromising the rate performance. In particular, with MRC/MRT or ZF processing, the effects of loop interference and hardware impairments at the relay can be eliminated for both DF and AF schemes if the power scaling coefficients satisfy $a+c < 1, b+c < 1, 0 \leq a, b < 1$ and $0 < c < 1$. Numerical results have showed that, in the aspect of enhancing the system performance, the hardware quality of sources and destinations has a greater impact than the hardware quality of the relay if the loop interference is small. In addition, performance improvement is larger with ZF processing than with the MRC/MRT processing if high-quality hardware is used at the sources and destinations. On the other hand, the hardware quality of sources and destinations has basically the same impact as the hardware quality of the relay when the loop interference is large. Under both DF and AF schemes, using very large antenna arrays at the relay can suppress the impact of loop interference,

and MRC/MRT processing suppresses the impact of loop interference better than ZF processing.

APPENDIX A

First, we consider the distortion noises at the sources and the relay station. One has

$$\delta_{1,n} = \lambda_1 P_{\mathrm{S}} \mathbb{E}\left\{|x_n[i]|^2\right\} = \lambda_1 P_{\mathrm{S}} \tag{207}$$

$$\begin{aligned}\delta_{2,m} &= \mu_1 \mathbb{E}\left\{\left|y_{\mathrm{R},m}[i]\right|^2\right\} \\ &= \mu_1 \left((1+\lambda_1)P_{\mathrm{S}} \sum_{j=1}^{N} \beta_{\mathrm{SR},j} + (1+\lambda_2)P_{\mathrm{R}}\sigma_{\mathrm{LI}}^2 + 1\right)\end{aligned} \tag{208}$$

$$\delta_{3,m} = \lambda_2 P_{\mathrm{R}} \mathbb{E}\left\{|s_m[i]|^2\right\} = \frac{\lambda_2 P_{\mathrm{R}}}{N_{\mathrm{tx}}}. \tag{209}$$

By substituting (207), (208) and (209) into (9), (10) and (11), respectively, one obtains the complete statistical characterizations of $\mathbf{n}_1[i]$, $\mathbf{n}_2[i]$ and $\mathbf{n}_3[i]$.

When the relay uses an MRC receiver to process the received signal, the linear receiver matrix is given by $\mathbf{W} = \hat{\mathbf{G}}_{\mathrm{SR}}$. Then, the terms in $\mathrm{SINR}_{\mathrm{SR},n}^{\mathrm{MR}}$ are given as

$$A_{\mathrm{SR},n} = \mathbb{E}\left\{\left\|\mathbf{g}_{\mathrm{SR},n}\right\|^2\right\} = N_{\mathrm{rx}}\beta_{\mathrm{SR},n}. \tag{210}$$

$$\begin{aligned}B_{\mathrm{SR},n} &= \mathbb{E}\left\{\left|\hat{\mathbf{g}}_{\mathrm{SR},n}^H \mathbf{g}_{\mathrm{SR},n}\right|^2\right\} - \mathbb{E}\left\{\hat{\mathbf{g}}_{\mathrm{SR},n}^H \mathbf{g}_{\mathrm{SR},n}\right\}^2 \\ &= N_{\mathrm{rx}}\vartheta_{\mathrm{SR},nn} - N_{\mathrm{rx}}^2\beta_{\mathrm{SR},n}^2.\end{aligned} \tag{211}$$

where $\vartheta_{\mathrm{SR},nn}$ is defined in (121).

$$C_{\mathrm{SR},n} = \sum_{j\neq n}^{N} \mathbb{E}\left\{\left|\hat{\mathbf{g}}_{\mathrm{SR},n}^H \mathbf{g}_{\mathrm{SR},j}\right|^2\right\} = \sum_{j\neq n}^{N} N_{\mathrm{rx}}\vartheta_{\mathrm{SR},jn}. \tag{212}$$

$$D_{\mathrm{SR},n} = \lambda_1 P_{\mathrm{S}}(A_{\mathrm{SR},n}^2 + B_{\mathrm{SR},n} + C_{\mathrm{SR},n}). \tag{213}$$

$$\begin{aligned}E_{\mathrm{SR},n} &= \alpha_{\mathrm{MRT}}^2 \sum_{j=1}^{N} \sigma_{\mathrm{RD},j}^2 \mathbb{E}\left\{\hat{\mathbf{g}}_{\mathrm{SR},n}^H \mathbf{G}_{\mathrm{LI}}\mathbf{G}_{\mathrm{LI}}^H \hat{\mathbf{g}}_{\mathrm{SR},n}\right\} \\ &= \alpha_{\mathrm{MRT}}^2 N_{\mathrm{tx}} \sum_{j=1}^{N} \sigma_{\mathrm{RD},j}^2 \sigma_{\mathrm{LI}}^2 \mathbb{E}\left\{\hat{\mathbf{g}}_{\mathrm{SR},n}^H \hat{\mathbf{g}}_{\mathrm{SR},n}\right\} \\ &= N_{\mathrm{rx}}\sigma_{\mathrm{LI}}^2\sigma_{\mathrm{SR},n}^2.\end{aligned} \tag{214}$$

$$\begin{aligned}F_{\mathrm{SR},n} &= \mathbb{E}\left\{\hat{\mathbf{g}}_{\mathrm{SR},n}^H \mathbf{G}_{\mathrm{LI}}\mathbf{n}_3[i]\mathbf{n}_3^H[i]\mathbf{G}_{\mathrm{LI}}^H \hat{\mathbf{g}}_{\mathrm{SR},n}\right\} \\ &= \frac{\lambda_2 P_{\mathrm{R}}}{N_{\mathrm{tx}}} \mathbb{E}\left\{\hat{\mathbf{g}}_{\mathrm{SR},n}^H \mathbf{G}_{\mathrm{LI}}\mathbf{G}_{\mathrm{LI}}^H \hat{\mathbf{g}}_{\mathrm{SR},n}\right\} \\ &= N_{\mathrm{rx}}P_{\mathrm{R}}\lambda_2\sigma_{\mathrm{LI}}^2\sigma_{\mathrm{SR},n}^2.\end{aligned} \tag{215}$$

$$\begin{aligned}G_{\mathrm{SR},n} &= \mathbb{E}\left\{\left|\hat{\mathbf{g}}_{\mathrm{SR},n}^H \mathbf{n}_2[i]\right|^2\right\} = N_{\mathrm{rx}}\sigma_{\mathrm{SR},n}^2\mu_1 \\ &\quad \times \left(P_{\mathrm{S}}(1+\lambda_1)\sum_{j=1}^{N}\beta_{\mathrm{SR},j} + P_{\mathrm{R}}(1+\lambda_2)\sigma_{\mathrm{LI}}^2 + 1\right).\end{aligned} \tag{216}$$

$$H_{\mathrm{SR},n} = \mathbb{E}\left\{\left\|\hat{\mathbf{g}}_{\mathrm{SR},n}^H\right\|^2\right\} = N_{\mathrm{rx}}\sigma_{\mathrm{SR},n}^2. \tag{217}$$

Substituting (210) to (217) into (29) results in $\mathrm{SINR}_{\mathrm{SR},n}^{\mathrm{MR}}$. Following the same methodology as the one used to compute the expression of $\mathrm{SINR}_{\mathrm{SR},n}^{\mathrm{MR}}$, we can obtain $\mathrm{SINR}_{\mathrm{RD},n}^{\mathrm{MR}}$.

Finally, using the computed $\mathrm{SINR}_{\mathrm{SR},n}^{\mathrm{MR}}$ and $\mathrm{SINR}_{\mathrm{RD},n}^{\mathrm{MR}}$, we arrive at (43).

APPENDIX B

Similar to Appendix A, we consider first the distortion noises at the sources, the relay's receiver and the relay's transmitter, and can obtain the identical statistical characterizations of $\mathbf{n}_1[i]$, $\mathbf{n}_2[i]$ and $\mathbf{n}_3[i]$ as in Appendix A.

For convenience, we define

$$\mathbf{X}_{\mathrm{SR},1} = \mathbf{G}_{\mathrm{SR}} + \frac{\left(\mathbf{N}_{\mu,\mathrm{SR}} + \mathbf{N}_{\mathrm{r,P}}\right)\Phi_{\mathrm{SR}}^H}{\tau\sqrt{P_{\mathrm{P}}}} \tag{218}$$

$$\mathbf{X}_{\mathrm{SR},2} = \frac{\mathbf{G}_{\mathrm{SR}}\mathbf{N}_{\lambda,\mathrm{SR}}\Phi_{\mathrm{SR}}^H}{\tau\sqrt{P_{\mathrm{P}}}}. \tag{219}$$

We know that the entries of $\mathbf{X}_{\mathrm{SR},2}$ are i.i.d. $\mathcal{CN}\left(0, \frac{\lambda_{\mathrm{P}}}{\tau}\sum_{j=1}^{N}\beta_{\mathrm{SR},j}\right)$ random variables. When $0 \leq \frac{\lambda_{\mathrm{P}}}{\tau}\sum_{j=1}^{N}\beta_{\mathrm{SR},j} \leq 1$, we have [41]

$$\begin{aligned}\mathbf{W} &= \hat{\mathbf{G}}_{\mathrm{SR}}\left(\hat{\mathbf{G}}_{\mathrm{SR}}^H\hat{\mathbf{G}}_{\mathrm{SR}}\right)^{-1} \\ &\approx \mathbf{X}_{\mathrm{SR},1}^{\dagger} - \mathbf{X}_{\mathrm{SR},1}^{\dagger}\mathbf{X}_{\mathrm{SR},2}^H\mathbf{X}_{\mathrm{SR},1}^{\dagger}\end{aligned} \tag{220}$$

where

$$\mathbf{X}_{\mathrm{SR},1}^{\dagger} = \mathbf{X}_{\mathrm{SR},1}\left(\mathbf{X}_{\mathrm{SR},1}^H\mathbf{X}_{\mathrm{SR},1}\right)^{-1}. \tag{221}$$

From (220), different terms of $\mathrm{SINR}_{\mathrm{SR},n}^{\mathrm{ZF}}$ are given as [6]

$$A_{\mathrm{SR},n} = \mathbb{E}\left\{\mathbf{w}_n^H\mathbf{g}_{\mathrm{SR},n}\right\} = \theta_{\mathrm{SR},n}. \tag{222}$$

$$\begin{aligned}B_{\mathrm{SR},n} &= \mathbb{E}\left\{\left|\mathbf{w}_n^H\mathbf{g}_{\mathrm{SR},n}\right|^2\right\} - \mathbb{E}\left\{\mathbf{w}_n^H\mathbf{g}_{\mathrm{SR},n}\right\}^2 \\ &= \xi_{\mathrm{SR},nn} - \theta_{\mathrm{SR},n}^2.\end{aligned} \tag{223}$$

$$C_{\mathrm{SR},n} = \sum_{j\neq n}^{N}\mathbb{E}\left\{\left|\mathbf{w}_n^H\mathbf{g}_{\mathrm{SR},j}\right|^2\right\} = \sum_{j\neq n}^{N}\xi_{\mathrm{SR},jn}. \tag{224}$$

$$D_{\mathrm{SR},n} = \lambda_1 P_{\mathrm{S}}(A_{\mathrm{SR},n}^2 + B_{\mathrm{SR},n} + C_{\mathrm{SR},n}). \tag{225}$$

$$E_{\mathrm{SR},n} = \mathbb{E}\left\{\left\|\mathbf{w}_n^H\mathbf{G}_{\mathrm{LI}}\mathbf{A}\right\|^2\right\} = \sigma_{\mathrm{LI}}^2\varphi_{\mathrm{SR},n}. \tag{226}$$

$$F_{\mathrm{SR},n} = \mathbb{E}\left\{\left|\mathbf{w}_n^H\mathbf{G}_{\mathrm{LI}}\mathbf{n}_3[i]\right|^2\right\} = \lambda_2\sigma_{\mathrm{LI}}^2\varphi_{\mathrm{SR},n}P_{\mathrm{R}}. \tag{227}$$

$$\begin{aligned}G_{\mathrm{SR},n} &= \mathbb{E}\left\{\left|\mathbf{w}_n^H\mathbf{n}_2[i]\right|^2\right\} \\ &= \mu_1\varphi_{\mathrm{SR},n}\left(\begin{matrix}P_{\mathrm{S}}(1+\lambda_1)\sum_{j=1}^{N}\beta_{\mathrm{SR},j} \\ +P_{\mathrm{R}}(1+\lambda_2)\sigma_{\mathrm{LI}}^2 + 1\end{matrix}\right).\end{aligned} \tag{228}$$

$$H_{\mathrm{SR},n} = \mathbb{E}\left\{\left\|\mathbf{w}_n^H\right\|^2\right\} = \varphi_{\mathrm{SR},n}. \tag{229}$$

Substituting (222) to (229) into (29) yields $\mathrm{SINR}_{\mathrm{SR},n}^{\mathrm{ZF}}$. Following the similar method in (220), one has [41]

$$\begin{aligned}\mathbf{A} &= \alpha_{\mathrm{ZF}}\mathbf{A}_{\mathrm{ZF}}\\ &= \alpha_{\mathrm{ZF}}\hat{\mathbf{G}}_{\mathrm{RD}}^{*}\left(\hat{\mathbf{G}}_{\mathrm{RD}}^{T}\hat{\mathbf{G}}_{\mathrm{RD}}^{*}\right)^{-1}\\ &\approx \alpha_{\mathrm{ZF}}\left(\mathbf{X}_{\mathrm{RD},1}^{\dagger\dagger} - \mathbf{X}_{\mathrm{RD},1}^{\dagger\dagger}\mathbf{X}_{\mathrm{RD},2}^{T}\mathbf{X}_{\mathrm{RD},1}^{\dagger\dagger}\right)\end{aligned} \tag{230}$$

where

$$\mathbf{X}_{\mathrm{RD},1} = \mathbf{G}_{\mathrm{RD}} + \frac{\left(\mathbf{N}_{\mu,\mathrm{RD}} + \mathbf{N}_{\mathrm{t,P}}\right)\Phi_{\mathrm{RD}}^{H}}{\tau\sqrt{P_{\mathrm{P}}}} \tag{231}$$

$$\mathbf{X}_{\mathrm{RD},2} = \frac{\mathbf{G}_{\mathrm{RD}}\mathbf{N}_{\lambda,\mathrm{RD}}\Phi_{\mathrm{RD}}^{H}}{\tau\sqrt{P_{\mathrm{P}}}} \tag{232}$$

$$\mathbf{X}_{\mathrm{RD},1}^{\dagger\dagger} = \mathbf{X}_{\mathrm{RD},1}^{*}\left(\mathbf{X}_{\mathrm{RD},1}^{T}\mathbf{X}_{\mathrm{RD},1}^{*}\right)^{-1}. \tag{233}$$

From (230), different terms of $\mathrm{SINR}_{\mathrm{RD},n}^{\mathrm{ZF}}$ are given as [6]

$$\alpha_{\mathrm{ZF}} = \frac{1}{\mathbb{E}\left\{\|\mathbf{A}_{\mathrm{ZF}}\|^2\right\}} = \sqrt{\frac{1}{\sum_{j=1}^{N}\varphi_{\mathrm{RD},j}}}. \tag{234}$$

$$A_{\mathrm{RD},n} = \mathbb{E}\left\{\mathbf{g}_{\mathrm{RD},n}^{T}\mathbf{a}_n\right\} = \alpha_{\mathrm{ZF}}\theta_{\mathrm{RD},n}. \tag{235}$$

$$\begin{aligned}B_{\mathrm{RD},n} &= \mathbb{E}\left\{\left|\mathbf{g}_{\mathrm{RD},n}^{T}\mathbf{a}_n\right|^2\right\} - \mathbb{E}\left\{\mathbf{g}_{\mathrm{RD},n}^{T}\mathbf{a}_n\right\}^2\\ &= \alpha_{\mathrm{ZF}}^2(\xi_{\mathrm{RD},nn} - \theta_{\mathrm{RD},n}^2).\end{aligned} \tag{236}$$

$$C_{\mathrm{RD},n} = \sum_{j\neq n}^{N}\mathbb{E}\left\{\left|\mathbf{g}_{\mathrm{RD},n}^{T}\mathbf{a}_j\right|^2\right\} = \alpha_{\mathrm{ZF}}^2\sum_{j\neq n}^{N}\xi_{\mathrm{RD},nj}. \tag{237}$$

$$D_{\mathrm{RD},n} = \mathbb{E}\left\{\left|\mathbf{g}_{\mathrm{RD},n}^{T}\mathbf{n}_3[i]\right|^2\right\} = \lambda_2\beta_{\mathrm{RD},n}P_{\mathrm{R}}. \tag{238}$$

$$\delta_{4,n} = \mu_2\left(P_{\mathrm{R}}\alpha_{\mathrm{ZF}}^2\sum_{j=1}^{N}\xi_{\mathrm{RD},nj} + P_{\mathrm{R}}\lambda_2\beta_{\mathrm{RD},n} + 1\right). \tag{239}$$

Substituting (234) to (239) into (38) gives $\mathrm{SINR}_{\mathrm{RD},n}^{\mathrm{ZF}}$. Then, using the computed $\mathrm{SINR}_{\mathrm{SR},n}^{\mathrm{ZF}}$ and $\mathrm{SINR}_{\mathrm{RD},n}^{\mathrm{ZF}}$, we arrive at (53).

APPENDIX C

Similar to the analysis of the DF scheme with MRC/MRT processing in Appendix A, the statistical properties of the distortion noises at the sources and the relay for the AF scheme with MRC/MRT processing are given as

$$\delta_{1,n} = \lambda_1 P_{\mathrm{S}}\mathbb{E}\left\{|x_n[i]|^2\right\} = \lambda_1 P_{\mathrm{S}} \tag{240}$$

$$\begin{aligned}\delta_{2,m} &= \mu_1\mathbb{E}\left\{\left|y_{\mathrm{R},m}[i]\right|^2\right\}\\ &= \mu_1\left((1+\lambda_1)P_{\mathrm{S}}\sum_{j=1}^{N}\beta_{\mathrm{SR},j} + (1+\lambda_2)P_{\mathrm{R}}\sigma_{\mathrm{LI}}^2 + 1\right)\end{aligned} \tag{241}$$

$$\delta_{3,m} = \lambda_2\mathbb{E}\left\{\left|y_{\mathrm{RT},m}[i]\right|^2\right\} = \frac{\lambda_2 P_{\mathrm{R}}}{N_{\mathrm{tx}}}. \tag{242}$$

where $y_{\mathrm{RT},m}[i]$ is the mth elements of $\mathbf{y}_{\mathrm{RT}}[i]$. By substituting (240), (241) and (242) into (9), (10) and (11), one obtains the complete statistical characterizations of $\mathbf{n}_1[i]$, $\mathbf{n}_2[i]$ and $\mathbf{n}_3[i]$.

When the relay employs MRC/MRT processing, the processing matrix at the relay is $\mathbf{F} = \hat{\mathbf{G}}_{\mathrm{RD}}^{*}\hat{\mathbf{G}}_{\mathrm{SR}}^{H}$. Let

$$W_1 = \mathbb{E}\left\{\|\mathbf{F}\|^2\right\} = N_{\mathrm{tx}}N_{\mathrm{rx}}\sum_{i=1}^{N}\sigma_{\mathrm{RD},i}^2\sigma_{\mathrm{SR},i}^2. \tag{243}$$

$$W_2 = \mathbb{E}\left\{\left\|\mathbf{g}_{\mathrm{RD},n}^{T}\mathbf{F}\right\|^2\right\} = N_{\mathrm{tx}}N_{\mathrm{rx}}\sum_{i=1}^{N}\vartheta_{\mathrm{RD},ni}\sigma_{\mathrm{SR},i}^2. \tag{244}$$

$$W_3 = \mathbb{E}\left\{\left\|\mathbf{F}\mathbf{g}_{\mathrm{SR},n}\right\|^2\right\} = N_{\mathrm{tx}}N_{\mathrm{rx}}\sum_{i=1}^{N}\vartheta_{\mathrm{SR},ni}\sigma_{\mathrm{RD},i}^2. \tag{245}$$

$$W_4 = \mathbb{E}\left\{\mathbf{g}_{\mathrm{RD},n}^{T}\mathbf{F}\mathbf{g}_{\mathrm{SR},n}\right\} = N_{\mathrm{tx}}N_{\mathrm{rx}}\beta_{\mathrm{RD},n}\beta_{\mathrm{SR},n}. \tag{246}$$

$$W_5 = \mathbb{E}\left\{\left|\mathbf{g}_{\mathrm{RD},n}^{T}\mathbf{F}\mathbf{g}_{\mathrm{SR},n}\right|^2\right\} = N_{\mathrm{tx}}N_{\mathrm{rx}}\sum_{i=1}^{N}\vartheta_{\mathrm{RD},ni}\vartheta_{\mathrm{SR},ni}. \tag{247}$$

$$W_6 = \mathbb{E}\left\{\left|\mathbf{g}_{\mathrm{RD},n}^{T}\mathbf{F}\mathbf{g}_{\mathrm{SR},j}\right|^2\right\} = N_{\mathrm{tx}}N_{\mathrm{rx}}\sum_{i=1}^{N}\vartheta_{\mathrm{RD},ni}\vartheta_{\mathrm{SR},ji}. \tag{248}$$

Based on (243) to (248), one has

$$E_{1,n} = \mathbb{E}\left\{\mathbf{g}_{\mathrm{RD},n}^{T}\mathbf{F}\mathbf{g}_{\mathrm{SR},n}\right\} = W_4. \tag{249}$$

$$E_{2,n} = \mathbb{V}\mathrm{ar}\left(\mathbf{g}_{\mathrm{RD},n}^{T}\mathbf{F}\mathbf{g}_{\mathrm{SR},n}\right) = W_5 - W_4^2. \tag{250}$$

$$E_{3,n} = \sum_{j\neq n}^{N}\mathbb{E}\left\{\left|\mathbf{g}_{\mathrm{RD},n}^{T}\mathbf{F}\mathbf{g}_{\mathrm{SR},j}\right|^2\right\} = \sum_{j\neq n}^{N}W_6. \tag{251}$$

$$\begin{aligned}E_{4,n} &= \mathbb{E}\left\{\left|\mathbf{g}_{\mathrm{RD},n}^{T}\mathbf{F}\mathbf{G}_{\mathrm{SR}}\mathbf{n}_1[i-1]\right|^2\right\}\\ &= \lambda_1 P_{\mathrm{S}}\left(W_5 + \sum_{j\neq n}^{N}W_6\right).\end{aligned} \tag{252}$$

$$E_{5,n} = \mathbb{E}\left\{\left|\mathbf{g}_{\mathrm{RD},n}^{T}\mathbf{F}\mathbf{G}_{\mathrm{LI}}\tilde{\mathbf{y}}_{\mathrm{RT}}[i-1]\right|^2\right\} = \sigma_{\mathrm{LI}}^2 W_2. \tag{253}$$

$$E_{6,n} = \mathbb{E}\left\{\left|\mathbf{g}_{\mathrm{RD},n}^{T}\mathbf{F}\mathbf{G}_{\mathrm{LI}}\mathbf{n}_3[i-1]\right|^2\right\} = \lambda_2 P_{\mathrm{R}}\sigma_{\mathrm{LI}}^2 W_2. \tag{254}$$

$$E_{7,n} = \mathbb{E}\left\{\left|\mathbf{g}_{\mathrm{RD},n}^{T}\mathbf{F}\mathbf{n}_{\mathrm{R}}[i-1]\right|^2\right\} = W_2. \tag{255}$$

$$E_{8,n} = \mathbb{E}\left\{\left|\mathbf{g}_{\mathrm{RD},n}^{T}\mathbf{F}\mathbf{n}_2[i-1]\right|^2\right\} = \delta_{2,m}W_2. \tag{256}$$

$$E_{9,n} = \mathbb{E}\left\{\left|\mathbf{g}_{\mathrm{RD},n}^{T}\mathbf{n}_3[i]\right|^2\right\} = \lambda_2 P_{\mathrm{R}}\beta_{\mathrm{RD},n}. \tag{257}$$

Substituting $E_{k,n}$, $k = 1,\ldots,9$, ρ and $\delta_{4,n}$ into (107) results in (118), where ρ and $\delta_{4,n}$ are shown at top of the next page.

$$\rho = \sqrt{\frac{1}{\left(\delta_{2,m} + P_{\mathrm{R}}\left(1+\lambda_2\right)\sigma_{\mathrm{LI}}^2 + 1\right) W_1 + P_{\mathrm{S}}\left(1+\lambda_1\right)\sum\limits_{n=1}^{N} W_3}} \tag{258}$$

$$\delta_{4,n} = \mu_2 \left(\rho^2 P_{\mathrm{R}} P_{\mathrm{S}} \left(1+\lambda_1\right) \left(W_5 + \sum_{j \neq n}^{N} W_6 \right) + \left(\rho^2 P_{\mathrm{R}} \left(1+\delta_{2,m}\right) + \rho^2 P_{\mathrm{R}}^2 \left(1+\lambda_2\right)\sigma_{\mathrm{LI}}^2 \right) W_2 + P_{\mathrm{R}} \lambda_2 \beta_{\mathrm{RD},n} + 1 \right) \tag{259}$$

APPENDIX D

Similar to the analysis of the AF scheme with MRC/MRT processing in Appendix C, the distortion noises at the sources, the relay's receiver and the relay's transmitter for the AF scheme with ZF processing have the same statistical properties of $\mathbf{n}_1[i]$, $\mathbf{n}_2[i]$ and $\mathbf{n}_3[i]$ as in Appendix C.

With ZF processing, the processing matrix at the relay is $\mathbf{F} = \hat{\mathbf{G}}_{\mathrm{RD}}^{*}\left(\hat{\mathbf{G}}_{\mathrm{RD}}^{T}\hat{\mathbf{G}}_{\mathrm{RD}}^{*}\right)^{-1}\left(\hat{\mathbf{G}}_{\mathrm{SR}}^{H}\hat{\mathbf{G}}_{\mathrm{SR}}\right)^{-1}\hat{\mathbf{G}}_{\mathrm{SR}}^{H}$. Following similar derivations in (220) and (230), one obtains [41]

$$\begin{aligned}\mathbf{F} &= \hat{\mathbf{G}}_{\mathrm{RD}}^{*}\left(\hat{\mathbf{G}}_{\mathrm{RD}}^{T}\hat{\mathbf{G}}_{\mathrm{RD}}^{*}\right)^{-1}\left(\hat{\mathbf{G}}_{\mathrm{SR}}^{H}\hat{\mathbf{G}}_{\mathrm{SR}}\right)^{-1}\hat{\mathbf{G}}_{\mathrm{SR}}^{H} \\ &\approx \left(\mathbf{X}_{\mathrm{RD},1}^{\dagger\dagger} - \mathbf{X}_{\mathrm{RD},1}^{\dagger\dagger}\mathbf{X}_{\mathrm{RD},2}^{T}\mathbf{X}_{\mathrm{RD},1}^{\dagger\dagger}\right) \\ &\quad \times \left(\mathbf{X}_{\mathrm{SR},1}^{\dagger} - \mathbf{X}_{\mathrm{SR},1}^{\dagger}\mathbf{X}_{\mathrm{SR},2}^{H}\mathbf{X}_{\mathrm{SR},1}^{\dagger}\right)^{H}.\end{aligned} \tag{260}$$

Based on (260), one has [6]

$$W_1 = \mathbb{E}\left\{\|\mathbf{F}\|^2\right\} = \sum_{i=1}^{N}\varphi_{\mathrm{RD},i}\varphi_{\mathrm{SR},i}. \tag{261}$$

$$W_2 = \mathbb{E}\left\{\left\|\mathbf{g}_{\mathrm{RD},n}^{T}\mathbf{F}\right\|^2\right\} = \sum_{i=1}^{N}\xi_{\mathrm{RD},ni}\varphi_{\mathrm{SR},i}. \tag{262}$$

$$W_3 = \mathbb{E}\left\{\left\|\mathbf{F}\mathbf{g}_{\mathrm{SR},n}\right\|^2\right\} = \sum_{i=1}^{N}\xi_{\mathrm{SR},ni}\varphi_{\mathrm{RD},i}. \tag{263}$$

$$W_4 = \mathbb{E}\left\{\mathbf{g}_{\mathrm{RD},n}^{T}\mathbf{F}\mathbf{g}_{\mathrm{SR},n}\right\} = \theta_{\mathrm{RD},n}\theta_{\mathrm{SR},n}. \tag{264}$$

$$W_5 = \mathbb{E}\left\{\left|\mathbf{g}_{\mathrm{RD},n}^{T}\mathbf{F}\mathbf{g}_{\mathrm{SR},n}\right|^2\right\} = \sum_{i=1}^{N}\xi_{\mathrm{RD},ni}\xi_{\mathrm{SR},ni}. \tag{265}$$

$$W_6 = \mathbb{E}\left\{\left|\mathbf{g}_{\mathrm{RD},n}^{T}\mathbf{F}\mathbf{g}_{\mathrm{SR},j}\right|^2\right\} = \sum_{i=1}^{N}\xi_{\mathrm{RD},ni}\xi_{\mathrm{SR},ji}. \tag{266}$$

Finally, substituting W_k, $k = 1, \ldots, 6$ into (249) to (259), and using the same method in Appendix C, we can obtain the expression of $\mathbf{S}_{\mathrm{FD,AF}}^{\mathrm{ZF}}$.

REFERENCES

[1] T. L. Marzetta, "Noncooperative cellular wireless with unlimited numbers of base station antennas," *IEEE Trans. Wireless Commun.*, vol. 9, no. 11, pp. 3590–3600, Nov. 2010.

[2] J. Hoydis, S. ten Brink, and M. Debbah, "Massive MIMO in the UL/DL of cellular networks: How many antennas do we need?" *IEEE J. Sel. Areas Commun.*, vol. 31, no. 2, pp. 160–171, Feb. 2013.

[3] F. Rusek *et al.*, "Scaling up MIMO: Opportunities and challenges with very large arrays," *IEEE Signal Process. Mag.*, vol. 30, no. 1, pp. 40–60, Jan. 2013.

[4] E. G. Larsson, O. Edfors, F. Tufvesson, and T. L. Marzetta, "Massive MIMO for next generation wireless systems," *IEEE Commun. Mag.*, vol. 52, no. 2, pp. 186–195, Feb. 2014.

[5] M. Shafi *et al.*, "5G: A tutorial overview of standards, trials, challenges, deployment, and practice," *IEEE J. Sel. Areas Commun.*, vol. 35, no. 6, pp. 1201–1221, Jun. 2017.

[6] H. Q. Ngo, E. G. Larsson, and T. L. Marzetta, "Energy and spectral efficiency of very large multiuser MIMO systems," *IEEE Trans. Commun.*, vol. 61, no. 4, pp. 1436–1449, Apr. 2013.

[7] A. He, L. Wang, Y. Chen, K.-K. Wong, and M. Elkashlan, "Spectral and energy efficiency of uplink D2D underlaid massive MIMO cellular networks," *IEEE Trans. Commun.*, vol. 65, no. 9, pp. 3780–3793, Sep. 2017.

[8] W. Liu, S. Han, and C. Yang, "Energy efficiency scaling law of massive MIMO systems," *IEEE Trans. Commun.*, vol. 65, no. 1, pp. 107–121, Jan. 2017.

[9] Y. Li, P. Fan, A. Leukhin, and L. Liu, "On the spectral and energy efficiency of full-duplex small-cell wireless systems with massive MIMO," *IEEE Trans. Veh. Technol.*, vol. 66, no. 3, pp. 2339–2353, Mar. 2017.

[10] Z. Liu, W. Du, and D. Sun, "Energy and spectral efficiency tradeoff for massive MIMO systems with transmit antenna selection," *IEEE Trans. Veh. Technol.*, vol. 66, no. 5, pp. 4453–4457, May 2017.

[11] Z. Zhang, X. Chai, K. Long, A. V. Vasilakos, and L. Hanzo, "Full duplex techniques for 5G networks: Self-interference cancellation, protocol design, and relay selection," *IEEE Commun. Mag.*, vol. 53, no. 5, pp. 128–137, May 2015.

[12] A. Sabharwal, P. Schniter, D. Guo, D. W. Bliss, S. Rangarajan, and R. Wichman, "In-band full-duplex wireless: Challenges and opportunities," *IEEE J. Sel. Areas Commun.*, vol. 32, no. 9, pp. 1637–1652, Sep. 2014.

[13] H. A. Suraweera, I. Krikidis, G. Zheng, C. Yuen, and P. J. Smith, "Low-complexity end-to-end performance optimization in MIMO full-duplex relay systems," *IEEE Trans. Wireless Commun.*, vol. 13, no. 2, pp. 913–927, Feb. 2014.

[14] M. Duarte, C. Dick, and A. Sabharwal, "Experiment-driven characterization of full-duplex wireless systems," *IEEE Trans. Wireless Commun.*, vol. 11, no. 12, pp. 4296–4307, Dec. 2012.

[15] X. Chen, L. Lei, H. Zhang, and C. Yuen, "Large-scale MIMO relaying techniques for physical layer security: AF or DF?" *IEEE Trans. Wireless Commun.*, vol. 14, no. 9, pp. 5135–5146, Sep. 2015.

[16] H. Q. Ngo, H. A. Suraweerat, M. Matthaiou, and E. G. Larsson, "Multipair massive MIMO full-duplex relaying with MRC/MRT processing," in *Proc. IEEE ICC*, Sydney, NSW, Australia, Jun. 2014, pp. 4807–4813.

[17] H. Q. Ngo, H. A. Suraweera, M. Matthaiou, and E. G. Larsson, "Multipair full-duplex relaying with massive arrays and linear processing," *IEEE J. Sel. Areas Commun.*, vol. 32, no. 9, pp. 1721–1737, Sep. 2014.

[18] X. Jia, P. Deng, L. Yang, and H. Zhu, "Spectrum and energy efficiencies for multiuser pairs massive MIMO systems with full-duplex amplify-and-forward relay," *IEEE Access*, vol. 3, pp. 1907–1918, 2015.

[19] X. Xia, Y. Xu, K. Xu, D. Zhang, and W. Ma, "Full-duplex massive MIMO AF relaying with semiblind gain control," *IEEE Trans. Veh. Technol.*, vol. 65, no. 7, pp. 5797–5804, Jul. 2016.

[20] Z. Zhang, Z. Chen, M. Shen, and B. Xia, "Spectral and energy efficiency of multipair two-way full-duplex relay systems with massive MIMO," *IEEE J. Sel. Areas Commun.*, vol. 34, no. 4, pp. 848–863, Apr. 2016.

[21] C. Kong, C. Zhong, S. Jin, S. Yang, H. Lin, and Z. Zhang, "Multipair full-duplex massive MIMO relaying with low-resolution ADCs and imperfect CSI," in *Proc. IEEE ICC*, Pairs, France, May 2017, pp. 1–6.

[22] C. Kong, C. Zhong, S. Jin, S. Yang, H. Lin, and Z. Zhang, "Full-duplex massive MIMO relaying systems with low-resolution ADCs," *IEEE Trans. Wireless Commun.*, vol. 16, no. 8, pp. 5033–5047, Aug. 2017.

[23] J. Feng, S. Ma, G. Yang, and B. Xia, "Power scaling of full-duplex two-way massive MIMO relay systems with correlated antennas and MRC/MRT processing," *IEEE Trans. Wireless Commun.*, vol. 16, no. 7, pp. 4738–4753, Jul. 2017.
[24] S. Wang, Y. Liu, W. Zhang, and H. Zhang, "Achievable rates of full-duplex massive MIMO relay systems over rician fading channels," *IEEE Trans. Veh. Technol.*, vol. 66, no. 11, pp. 9825–9837, Nov. 2017.
[25] X. Sun, K. Xu, W. Ma, Y. Xu, X. Xia, and D. Zhang, "Multi-pair two-way massive MIMO AF full-duplex relaying with imperfect CSI over Ricean fading channels," *IEEE Access*, vol. 4, pp. 4933–4945, 2016.
[26] E. Björnson, J. Hoydis, M. Kountouris, and M. Debbah, "Massive MIMO systems with non-ideal hardware: Energy efficiency, estimation, and capacity limits," *IEEE Trans. Inf. Theory*, vol. 60, no. 11, pp. 7112–7139, Nov. 2014.
[27] E. Björnson, M. Matthaiou, and M. Debbah, "Massive MIMO with non-ideal arbitrary arrays: Hardware scaling laws and circuit-aware design," *IEEE Trans. Wireless Commun.*, vol. 14, no. 8, pp. 4353–4368, Aug. 2015.
[28] S. Zarei, W. H. Gerstacker, J. Aulin, and R. Schober, "Multi-cell massive MIMO systems with hardware impairments: Uplink-downlink duality and downlink precoding," *IEEE Trans. Wireless Commun.*, vol. 16, no. 8, pp. 5115–5130, Aug. 2017.
[29] Y. Liu, X. Xue, J. Zhang, X. Li, L. Dai, and S. Jin, "Multipair massive MIMO two-way full-duplex relay systems with hardware impairments," in *Proc. IEEE GLOBECOM*, Singapore, Dec. 2017, pp. 1–6.
[30] J. Zhang, X. Xue, E. Björnson, B. Ai, and S. Jin, "Spectral efficiency of multipair massive MIMO two-way relaying with hardware impairments," *IEEE Wireless Commun. Lett.*, vol. 7, no. 1, pp. 14–17, Feb. 2018.
[31] X. Xia, D. Zhang, K. Xu, W. Ma, and Y. Xu, "Hardware impairments aware transceiver for full-duplex massive MIMO relaying," *IEEE Trans. Signal Process.*, vol. 63, no. 24, pp. 6565–6580, Dec. 2015.
[32] K. Xu, Y. Gao, W. Xie, X. Xia, and Y. Xu, "Achievable rate of full-duplex massive MIMO relaying with hardware impairments," in *Proc. IEEE PACRIM*, Victoria, BC, Canada, Aug. 2015, pp. 84–89.
[33] W. Xie, X. Xia, Y. Xu, K. Xu, and Y. Wang, "Massive MIMO full-duplex relaying with hardware impairments," *J. Commun. Netw.*, vol. 19, no. 4, pp. 351–362, Aug. 2017.
[34] M. Biguesh and A. B. Gershman, "Training-based MIMO channel estimation: A study of estimator tradeoffs and optimal training signals," *IEEE Trans. Signal Process.*, vol. 54, no. 3, pp. 884–893, Mar. 2006.
[35] G. Santella and F. Mazzenga, "A hybrid analytical-simulation procedure for performance evaluation in M-QAM-OFDM schemes in presence of nonlinear distortions," *IEEE Trans. Veh. Technol.*, vol. 47, no. 1, pp. 142–151, Feb. 1998.
[36] H. Suzuki, T. V. A. Tran, I. B. Collings, G. Daniels, and M. Hedley, "Transmitter noise effect on the performance of a MIMO-OFDM hardware implementation achieving improved coverage," *IEEE J. Sel. Areas Commun.*, vol. 26, no. 6, pp. 867–876, Aug. 2008.
[37] T. Riihonen, S. Werner, and R. Wichman, "Mitigation of loopback self-interference in full-duplex MIMO relays," *IEEE Trans. Signal Process.*, vol. 59, no. 12, pp. 5983–5993, Dec. 2011.
[38] J. Jose, A. Ashikhmin, T. L. Marzetta, and S. Vishwanath, "Pilot contamination and precoding in multi-cell TDD systems," *IEEE Trans. Wireless Commun.*, vol. 10, no. 8, pp. 2640–2651, Aug. 2011.
[39] A. Khansefid and H. Minn, "Achievable downlink rates of MRC and ZF precoders in massive MIMO with uplink and downlink pilot contamination," *IEEE Trans. Commun.*, vol. 63, no. 12, pp. 4849–4864, Dec. 2015.
[40] H. Q. Ngo and E. G. Larsson, "Large-scale multipair two-way relay networks with distributed AF beamforming," *IEEE Commun. Lett.*, vol. 17, no. 12, pp. 1–4, Dec. 2013.
[41] N. I. Miridakis, T. A. Tsiftsis, and C. Rowell, "Distributed spatial multiplexing systems with hardware impairments and imperfect channel estimation under rank-1 Rician fading channels," *IEEE Trans. Veh. Technol.*, vol. 66, no. 6, pp. 5122–5133, Jun. 2017.

SI-NIAN JIN received the B.S. degree in communication engineering from Shandong University, Weihai, China, in 2014, and the M.S. degree in information and communication engineering from Dalian Maritime University, Dalian, China, in 2017, where he is currently pursuing the Ph.D. degree in information and communication engineering. His research interests include massive MIMO systems and cooperative communications.

DIAN-WU YUE received the B.S. and M.S. degrees in mathematics from Nankai University, Tianjin, China, in 1986 and 1989, respectively, and the Ph.D. degree in communications and information engineering from the Beijing University of Posts and Telecommunications, Beijing, China, in 1996. From 1989 to 1993, he was a Research Assistant of applied mathematics with the Dalian University of Technology, Dalian, China. From 1996 to 2003, he was an Associate Professor of communications and information engineering with the Nanjing University of Posts and Telecommunications, Nanjing, China. From 2000 to 2001, he was a Visiting Scholar with the University of Manitoba, Winnipeg, MB, Canada. From 2001 to 2002, he was a Post-Doctoral Fellow with the University of Waterloo, Waterloo, ON, Canada. Since 2003, he has been a Full Professor of communications and information engineering with the Dalian Maritime University, Dalian, China. His current research interests include massive MIMO systems, millimeter-wave MIMO communications, and cooperative relaying communications.

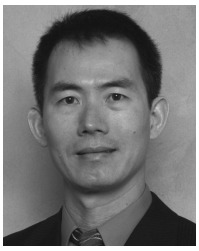

HA H. NGUYEN (M'01–SM'05) received the B.Eng. degree from the Hanoi University of Technology, Hanoi, Vietnam, in 1995, the M.Eng. degree from the Asian Institute of Technology, Bangkok, Thailand, in 1997, and the Ph.D. degree from the University of Manitoba, Winnipeg, MB, Canada, in 2001, all in electrical engineering. He joined the Department of Electrical and Computer Engineering, University of Saskatchewan, Saskatoon, SK, Canada, in 2001, and became a Full Professor in 2007. He is currently the Chair of Cisco Systems Research. He has co-authored with Ed Shwedyk the textbook *A First Course in Digital Communications* (Cambridge University Press). His research interests fall into broad areas of communication theory, wireless communications, and statistical signal processing. He is a fellow of the Engineering Institute of Canada and a Registered Member of the Association of Professional Engineers and Geoscientists of Saskatchewan. He was a Co-Chair of the Multiple Antenna Systems and Space-Time Processing Track, IEEE Vehicular Technology Conferences (Fall 2010, Ottawa, ON, Canada and Fall 2012, Quebec, QC, Canada), a Lead Co-Chair of the Wireless Access Track, IEEE Vehicular Technology Conferences (Fall 2014, Vancouver, BC, Canada), a Lead Co-Chair of the Multiple Antenna Systems and Cooperative Communications Track, IEEE Vehicular Technology Conference (Fall 2016, Montreal, QC, Canada), and a Technical Program Co-Chair of the Canadian Workshop on Information Theory (2015, St. John's, NL, Canada). He was an Associate Editor of the IEEE TRANSACTIONS ON WIRELESS COMMUNICATIONS from 2007 to 2011 and the IEEE WIRELESS COMMUNICATIONS LETTERS from 2011 to 2016. He currently serves as an Associate Editor of the IEEE TRANSACTIONS ON VEHICULAR TECHNOLOGY.